WAMBUA, DICKSON M., M.S. Gold Nanoparticle Enhanced Capillary Electrophoresis Separations for Alzheimer's Disease Biomarker Detection. (2009)
Supervised by Dr. G. B. Dawson. 92 pp.

Alzheimer's disease (AD) is a progressive, neurodegenerative disease characterized by memory and cognitive loss, the formation of senile plaques containing amyloid-beta (Aβ) peptides, degeneration of the cholinergic neurons and the development of neurofibrillary tangles in the brains of the affected people.[1] It is estimate that 5.1 million people in the United States are suffering from AD. The total annual care cost associated with AD is more than $ 148 billion and is constantly increasing[3]. Presently, there is no specific clinical test to diagnose AD, however, amyloid beta peptides and tau proteins have been shown to be reliable biomarkers that can be used for AD diagnosis and tracking disease progression.[5] It is important therefore that proper methods and techniques be devised for the identification, quantification and analysis of AD biomarkers to enable the reliable clinical diagnosis of the disease.

In this study, modified gold nanoparticles were used as a pseudo stationary phase in a capillary electrochromatography technique. An asymmetric disulfide synthesized from mercaptoundecanoic acid and dodecanethiol was chemisorbed onto 10 nm gold nanoparticles to form the pseudo stationary phase. With the help of the gold nanoparticle pseudo stationary phase, the separation of two Alzheimer's disease biomarkers namely; amyloid beta 40 and amyloid beta 42 was accomplished. This study demonstrates that the presence of modified gold nanoparticles in capillary electrochromatography can greatly influence the separation of amyloid beta peptides.

GOLD NANOPARTICLE ENHANCED CAPILLARY ELECTROPHORESIS SEPARATIONS FOR ALZHEIMER'S DISEASE BIOMARKER DETECTION

by

Dickson M. Wambua

A Thesis Submitted to
the Faculty of The Graduate School at
The University of North Carolina at Greensboro
in Partial Fulfillment
of the Requirements for the Degree
Master of Science

Greensboro
2009

Approved by

Dr. G. B. Dawson

_____

Committee Chair

To Sarah and Elizabeth

APPROVAL PAGE

This thesis has been approved by the following committee of the Faculty of The Graduate School at The University of North Carolina at Greensboro.

Committee Chair _____
Dr. G. B. Dawson

Committee Members _____
Dr. Nadja Cech

_____
Dr. Jason Reddick

_____
Date of Acceptance by Committee

_____
Date of Final Oral Examination

ACKNOWLEDGEMENTS

I would like to thank all the people who inspired me in my Masters Program. I especially want to offer my sincerest gratitude to my advisor Dr. G. B. Dawson who excellently guided me though my research work, patiently and with knowledge while allowing me the opportunity to work in my own way. Without him, this thesis would not have been accomplished.

Dr. Cech, Dr. Raner and Dr. Reddick deserve special thanks as my thesis committee members and advisors. They generously gave time to better my work; reading through my thesis drafts several times and providing new ideas and direction during my study.

I am grateful to the Department of Chemistry and Biochemistry for the teaching assistantship that supported me during my study at the University of North Carolina at Greensboro.

My thanks must go to the North Carolina Biotechnology Center – BRG Program for providing the financial support through which my research work was funded, and for the research assistantship position, that enabled me to concentrate more on the research.

I wish to extend my sincere thanks to my wife who persistently encouraged me to go back to school after years of working, and to the rest of my family for cheering me up continuously.

TABLE OF CONTENTS

LIST TABLES

Page

LIST OF FIGURES

Figure Page

CHAPTER I

INTRODUCTION

Statement of problem

Scientists estimate that 5.1 million people in the United States are suffering from Alzheimer's disease (AD). The total annual care cost associated with AD is more than $ 148 billion and is constantly increasing[3]. Presently, there is no specific clinical test to diagnose AD, however, amyloid beta (Aβ) peptides and tau proteins have been shown to be reliable biomarkers that can be used for AD diagnosis and tracking disease progression.[5] Our goal was to utilize a capillary electrochromatography technique and nanobiotechnology to achieve multi analyte analysis of AD biomarkers.

Objective 1

The first objective was the development of modified 10 nm gold nanoparticles as a pseudo stationary phase to be used in capillary electrochromatography for the separation of Alzheimer's disease biomarkers.

Asymmetric disulfides were synthesized and covalently linked to gold nanoparticles to form self assembled mixed monolayers capable of differentially interacting with Alzheimer's disease biomarkers. Figure 1 shows a modified gold nanoparticle.

Figure 1. Modified gold nanoparticle

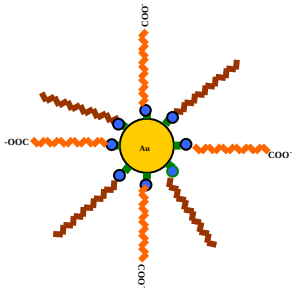

KEY

Yellow	= Gold nanoparticle
Light blue	= Sulfur atoms
Brown	= Carbon chain from dodecannethiol
Orange	= Carbon chain from mercaptoundecanoic

Objective 2

Our second objective was optimizing the separation of Alzheimer's disease biomarkers using modified gold nanoparticles as a capillary electrochromatography pseudo stationary phase.

Hypothesis

The presence of gold nanoparticles that are covalently modified with an asymmetric disulfide in a capillary electrophoresis separation buffer will allow the separation of amyloid beta peptides that are Alzheimer's disease biomarkers.

CHAPTER II

REVIEW OF THE LITERATURE

Alzheimer's disease

Alzheimer's disease (AD) is a progressive, neurodegenerative disease characterized by memory and cognitive loss, the formation of extracellular senile plaques (SP) containing amyloid - beta (Aβ) peptides, degeneration of the cholinergic neurons and the development of neurofibrillary tangles (NFT) composed of hyperphosphorylated forms of the tau protein in the brain.[1] These symptoms of AD are different from those observed in normal aging process. AD is increasingly becoming common in the aging population. It was estimated that in 2006, the global prevalence of AD was 26.6 million. With the increasing life expectancy and rise of an aging population, this figure is expected to quadruple by the year 2050, at which time it is estimated that 1 in 83 people in the world will be living with the disease. The Alzheimer's Association estimates that 5.1 million people in the United States suffer from AD. The total annual care cost is over $ 148 billion. If the current trends are not changed, this emergence of Alzheimer's disease will lead to a high negative social and economic impact. [2, 3]

The two major things that can be done to reverse this trend are: - i) people at high risk of AD need to be identified before the earliest symptoms become evident and ii) methods need to be developed that either reduce or slow the accumulation of AD neuropathology. Better diagnostic tools that will speed the diagnosis of Alzheimer's disease, formulation of medications or preventive measures are therefore needed.[2]

Alzheimer's disease is the most common type of dementia among the elderly population, with an average prevalence level of 1% at the age of 60, rising to 35% by the age of 90. Aging is clearly a major risk factor in the development of AD.[4]

According to the U.S. Department of Health and Human Services 2005-2006 progress report on Alzheimer's disease, there is no single specific clinical test that can diagnose AD, instead, many other causes of dementia must be ruled out first before clinical diagnosis of AD is made. For this kind of diagnosis, a detailed patient history is obtained thorough physical examination and cognitive assessments. Neuroimaging techniques have also been used to provide extra information to help in diagnosis, these include: - Computerized Tomography (CT), Magnetic Resonance Imaging (MRI), Single Photon Emission Computerized Tomography (SPECT) and Positron Emission Tomography (PET).[5] Definitive diagnosis of AD requires confirmation of the diagnosis by brain biopsy or autopsy, which shows the tangles and senile plaques that are a hallmark of AD.[6]

Although there has not been a proven available treatment that can reverse the neurodegenerative process, several disease modifying candidates are continuously being

put though clinical trials. The action of these drug candidates is based on the strength of several theories that have been advanced to explain the cause of AD.[5]

Theories advanced to explain the cause of AD

(i) The amyloid beta hypothesis

This hypothesis proposes that the excessive proteolytic cleavage of the Amyloid Precursor Protein (APP) by beta secretase and gamma secretase produces beta amyloid peptides. Beta secretase cleaves APP at NH_2 terminal domain while gamma secretase cleaves APP at C terminal domain, which results in many different peptides some of which have 40 or 42 amino acids, hence the terms Amyloid beta 40 (Aβ1-40) and Amyloid beta 42 (Aβ1-42) respectively.[7,8]

Many other proteases and peptidases have been shown to cleave APP, some of which perform the cleavage at multiple sites. These include Neprylisin, Plasmin, Insulin Degrading Enzyme, Endothelin Converting Enzyme, Angiotensin Converting Enzyme among others. Figure 2 below shows arrows indicating the possible cleavage sites of APP.

Figure 2. Cleavage sites of amyloid precursor protein

INITIAL	PROTEASE
N	Neprylisin
P	Plasmin
I	Insulin Degrading Enzyme
E	Endothelin Converting Enzyme
A	Angiotensin Converting Enzyme

Aβ-42 is however considered the major source of senile plaques and vascular deposits in the brains of AD patients. It is thought that Aβ peptides aggregate and form fibrils in the brain that lead to inflammations and neuronal loss, which is eventually associated with the progressive neurodegenerative nature of AD.[9]

The levels of Aβ1-40 and Aβ1-42 are thought to be important indicators of Alzheimer's disease and are widely accepted as reliable biomarkers for AD. Studies by Mayux *et al.* revealed that high baseline levels of these two peptides were a risk factor for the development of dementia. Their concentrations were particularly higher in people with abnormalities of processing APP due to a mutation, which can be tied to the early onset of familial AD.[11]

(ii) Phosphorylated tau and total tau hypothesis

Abundant quantities of Aβ have however been found in individuals that are cognitively sound, this observation led to the hypothesis that neurofibrillary tangles

formed by hyperphosphorylated tau could be the cause of AD as opposed to Aβ peptides.[12]

Tau is a microtubule associated protein involved in the assembly and stabilization of microtubules. Hyperphosphorylated tau is directly linked to the formation of neurofibrillary tangles in the brain; these tangles cause neuronal dysfunction and are a hallmark of AD. It is however not clearly understood whether the increased phosphorylation of tau is as a result of high activity of kinases or the down regulation of phosphatases.[10] Analysis of tau phosphorylated at serine 199 showed high specificity (85%) and sensitivity (85%) in differentiating between AD and other forms of dementia.[13]

Even with these developments in biomarker identification, the early diagnosis of AD and its differentiation from other forms of dementia remains very elusive at clinical levels, and the phenotypic characteristics of AD that include progressive loss of memory and degeneration of cognitive abilities are still the main diagnostic tools. It is however clear that a cascade of biochemical events begins long before these symptoms of AD can be observed .[14]

These studies clearly show that the quantitation of Aβ1-40, Aβ1-42, total tau or p-tau in CSF or plasma could hold a huge potential for the early diagnosis and the evaluation of progress of AD, these measurements in turn would spur the development of new therapies or vaccinations and development of new drugs.[15]

Analysis of Alzheimer's disease biomarkers

Several analytical techniques have been used for the analysis of Aβ1-40, Aβ1-42 and tau. The most commonly used method is the enzyme linked immunosorbent assay (ELISA) also known as enzyme immunoassay (EIA). This test is an immunochemical technique that has been used widely for the detection of antibodies. An antigen is first immobilized onto a solid surface then it is complexed with an antibody that is linked with an enzyme. Non specific binding is washed off and detection is achieved by incubating the enzyme-complex with a substrate that is converted into a detectable product. The detection instrument could be a fluorometer, spectrophotometer or a luminometer. [10]

ELISA has been used for the determination of the concentration of amyloid beta peptides ending at the amino acid position 42 ($A\beta_{x-42}$) in the undiluted cerebrospinal fluid of patients. It has also been used for the analysis of amyloid beta peptides from the brain extracts of patients.[15] Typical procedures for extraction of these biomarkers can however lead to formation of secondary structures of the peptides affecting the hybridization of the peptides onto the immobilized probes, a factor that can hinder the reliability of ELISA.[16]

Clarke *et al.* demonstrated that it is possible to detect the cellular levels of Aβ-40 and Aβ-42 directly from cell lysates. They used two a dimensional chromatography where size exclusion chromatography was first done to separate the contents of the lysates by molecular weight; a sample pre-concentration was then followed by separation using microbore liquid chromatography. Detection was done using electrospray-mass spectrometry (ESI-MS). The use of ESI-MS as a detection tool gave more flexibility to

the analysis and resulted in greater structural information from the samples compared to ELISA. [31]

Several studies have been done using capillary electrophoresis for the detection and quantitation of AD biomarker. Kato *et al.* developed a fast analytical method to separate a mixture of Aβ1-41 and Aβ1-42 fibrils in 5 minutes using capillary electrophoresis and a laser induced fluorescence detector (CE-LIF). The method was also found to be applicable for high throughput analysis of promising therapeutic agents of the disease. Patient samples are however complex and more sample cleanup procedures have to be developed for the method to be used for clinical diagnosis.[17]

Although traditional CE is fast and highly efficient in many circumstances, it poses a problem when small capillaries are used. This drawback is due to the low sensitivity resulting from absorbance detectors caused by the shorter path length available with small diameter capillaries. One of the major advantages of using larger diameter capillaries is to boost the technique's sensitivity which is enhanced through the longer path length. However, increase in inner diameters is associated with increased Joule heating due to the reduced surface area to volume ratio of the capillary at higher currents. The large capillaries cannot dissipate heat very fast and this leads to band broadening and poor resolution. [42]

Electrophoresis

Capillary electrophoresis

In recent years, Capillary Electrophoresis (CE) has emerged as a powerful technique for the separation of mixtures; this characteristic is attributed to its high separation speeds and the ability to use very small volumes of samples in the nanoliter range, while offering extremely high power of resolution.[19]

Electrophoresis is the differential migration of ions by attraction or repulsion in an electric field. CE is based on the differential migration of charged species through a silica capillary. The ends of the capillary are placed in buffer reservoirs with electrodes which are connected to a source of high voltage. Samples are introduced into the capillary usually at the anodic end either electrokinetically or hydrodynamically. High voltage is then applied across the capillary to perform the separation. The migration of analytes is caused by electroosmotic flow (EOF) and electrophoretic flow in the presence of a separation buffer. Detection can be done online or off-line at the cathodic end. Typically, capillaries of 50-100 µm internal diameter are used, although smaller and larger capillaries are commercially available and can also be used. Most capillaries used in CE are made of fused silica which means that the inside surface of the capillary is covered with negatively charged silanol groups when the electrolyte pH is above 3.

In the presence of a buffer, two inner layers of cations are formed, one of which is highly attracted to the negatively charged silanol groups and is referred to as a fixed layer. Another layer further from the silanol groups also forms and is attracted by the cathode's negative charge, this layer is mobile and is the source of electroosmotic flow.

When a potential difference is applied across the capillary, the cations in the mobile layer migrate towards the cathode, dragging along with them the solvent. This movement ensures that the bulk of the cations and electrophoresis buffer move towards the cathode. This resulting EOF is so strong that it overcomes the electrophoretic mobility and therefore all charged species and neutral compounds move towards the cathode. The charged species migrate at different speeds due to the difference in electrophoretic mobility, they are therefore separated according to their charge to size ratios. All neutral analytes and ions with equal mobilities do not experience the differential migration and thus cannot be separated by traditional capillary electrophoresis.[20]

Capillary electrochromatography

The failure of CE to separate neutral analytes is however a more challenging drawback. This situation has been overcome by the introduction of stationary phases that have now bridged electrophoresis and chromatography to make capillary electrochromatography (CEC). CEC is a variant of high performance liquid chromatography in which the flow of mobile phase is effected by the use of electroosmotic flow (EOF). Just like in CE, CEC is also performed in capillary tubes of 50-100 µm in diameter, the main difference is that CEC is performed either in a capillary packed with a stationary phase or a coated open tubular capillary. Application of a large voltage across the capillary generates EOF, the analytes are then partitioned between the stationary phase and the mobile phase. Charged analytes are separated according to

differences in partitioning as well as their electrophoretic mobility while neutral analytes separate due to differences in their extents of partitioning into the stationary phase.[18]

Micellar electrokinetic chromatography (MEKC)

The main problem of CEC is the development of backpressure. This can be solved by the introduction of a pseudo stationary phase instead of a fixed stationary phase. The use of pseudo stationary phase of micelles was first introduced by Terabe *et al.* The technique was named micellar electrokinetic chromatography (MEKC) and uses the same instrumentation as CE and CEC. In MEKC, the stationary phase is not permanently fixed, therefore the technique benefits from the fast regeneration of the column and does not experience stationary phase carry over effects like in CEC, furthermore, there are no complicated packing procedures and the column can easily be exchanged.[18,21]

Separation is based on the principle of partitioning analytes between a micelle phase and an aqueous phase. This partitioning is achieved by using ionic micellar solutions for separation. A widely used surfactant is sodium dodecyl sulfate (SDS). Above the critical micellar concentration, the surfactant aggregates to form micelles that act as a pseudo stationary phase with an outer polar surface and an inner hydrophobic core. Analytes in solution partition themselves between the micelles and the hydrophilic electrophoretic buffer, with the more hydrophobic analytes solubilizing into the micelle core while the hydrophilic analytes remain in the aqueous buffer solution. [21]

When neutral analytes are injected into the capillary and the electrophoresis potential difference is applied, the anionic nature of the surfactant enables the micelles to

have electrophoretic mobility that is counter to the EOF, however, since EOF is stronger than electrophoretic mobility, and the net movement is towards the cathode. Analytes solubilized in the micelle migrate slowly at the velocity of the micelle while the rest of the analytes free from the micelle migrate at the EOF velocity. Since the partitioning into the micelles is determined by the extend of hydrophobic interaction between the analytes and the micelles, the order of migration is similar to that of reverse phase liquid chromatography. Hydrophobicity and charge interactions of analytes at the surface of the micelles are thus the major factors that determine the separation of analytes.[21]

Many other approaches have been used in order to improve selectivity, sensitivity and reproducibility of capillary electrophoresis. Most of these involve the use of pseudo stationary phases. CE can therefore be divided into four major groups that include open tubular, packed column, monolithic and pseudo stationary phase CE.[22]

Detection methods and peptide derivatization

In capillary electrophoresis, samples are detected on-column at some point towards the end of the capillary. A small section of the protective polymer coating of the fused silica capillary can be burned off to expose an on column cell through which detection can be done. Ultraviolet/Visible (UV-Vis) absorbance is the most common means of detection. Although UV-Vis absorbance detection is very reliable, it is limited to analytes that have a chromophore. The sensitivity of UV-Vis detectors is proportional to the detection path length across the capillary cell. Since most capillaries used in capillary electrophoresis are in the range of 20-100 µm inner diameters, the detection

path length is small and the absorbance sensitivity becomes poor as the path length reduces with reducing capillary diameter. This loss of sensitivity leads to a poor limit of detection. Other methods of detection have also been used in capillary electrophoresis including mass spectrometry, chemiluminescence, electrochemical detection and fluorescence.[50]

Laser induced fluorescence detectors have very low limits of detection in the attomole to femtomole range. Non fluorescent analytes are covalently labeled with a fluorophore to enhance detection sensitivity. Excitation radiation is focused on the capillary cell where the polymer coating has been burned off. The resulting fluorescence is collected at 90° relative to the excitation beam.[51]

Since the β-amyloid peptides do not naturally fluoresce, derivatization to form fluorophores is a necessary step towards detection. ATTO-TAG FQ™ (3-(2-furoyl) quinoline-2-carboxaldehyde 2) has been widely used as a derivatization reagent for peptide tagging. An example of peptide derivatization using ATTO-TAG™ FQ is shown below in Figure 3.

Figure 3. Peptide derivatization using ATTO-TAG FQ™

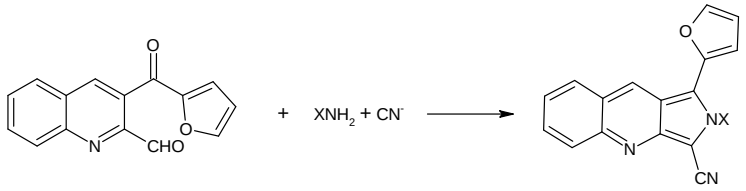

ATTO-TAG FQ™ Cyanoisoindole derivative

ATTO-TAG FQ™ specifically reacts with primary amines and even hydrophilic peptides. The resulting fluorescent cyanoisoindole derivatives can be excited by the 488 nm line of argon-ion laser with resultant emission maxima of ~590 nm. The limit of detection is in the attomole range (10^{-18} moles).[32] Parameters that play a role in CEC separations e.g. pH, buffer type and its concentration, electrophoresis voltage, and length of capillaries and laser power have to be optimized in order to achieve fast, accurate and precise separations with reproducible migration times.[49]

Joule heating and zwitterionic buffers

Band broadening in capillary electrophoresis is caused by many factors including length of injection zone, width of detector, Joule heating, electroosmotic flow and analyte-wall interactions. Joule heating is the result of heat generated by the passage of electrical current through a capillary filled with buffer; it plays a significant role in band broadening. When the heat generation exceeds heat dissipation, then a temperature gradient within the capillary occurs. The amount of heat produced depends on capillary dimensions and the type of buffer used. Generally, larger diameter capillaries have a small surface area to volume ratio and cannot dissipate heat as efficiently as smaller capillaries whose surface area to volume ratio is relatively higher. Large diameter capillaries therefore tend to generate more heat. High conductivity buffers exhibit high currents and contribute positively towards Joule heating. The use of very high voltage for electrophoresis also increases Joule heating.[42,43]

The temperature gradient due to Joule heating is both radial and axial and affects factors like electrical conductivity, diffusion coefficient and buffer viscosity. Changes in these factors lead to the non uniformity of electroosmotic flow, electrophoretic mobility and molecular diffusion causing a difference in the migration time of similar analytes that in turn causes band broadening and irreproducible migration times. [43]

Several ways exist in which Joule heating can be reduced. The use of capillaries with smaller internal diameters remarkably increases the surface area that is used for heat dissipation and dramatically decreases the overall current. This modification has the disadvantage of shortening the path length used for analyte detection and therefore becomes problematic especially for absorbance based detectors whose sensitivity is not very high. Another way of reducing Joule heating is by reducing the conductivity of the buffer by lowering its ionic strength thereby producing lesser current and heat; however with a decrease in ionic strength, analytes tend to adsorb more on the capillary wall. The electrophoresis voltage can also be lowered with the consequential decrease in efficiency and resolution of separation. [44]

One of the best ways to reduce Joule heating is by the use of zwitterionic buffers. These buffers have minimal charge and therefore generate very little current while still offering good conductivity. Furthermore, the low conductivity also reduces the negative effect of buffer depletion leading to longer and more stable operation time. Examples of zwitterionic buffers include tricine, bicine, HEPES (4-(2-hydroxyethyl)-1-piperazineethanesulfonic acid), CAPS (*N*-cyclohexyl-3-aminopropanesulfonic acid),

MES (2-(*N*-morpholino) ethanesulfonic acid) and tri (tris (hydroxymethyl) aminomethane). [45]

The pH of the running buffer is also a major factor in the efficiency of CE separations. At low pH, only a small proportion of the silanol groups on the capillary wall are ionized, therefore the electroosmotic force is low and migration times are long. The electroosmotic flow increases with increasing pH until all the available silanol groups on the capillary have been ionized, consequently very high pH buffers cause high electroosmotic flow and a very fast movement of analytes which may cause poor resolution. High buffer pH may however be beneficial for peptide and protein separation. Performing separations for samples with basic amino acids e.g. lysine at pH ranges above the pKa of the amino acid residues ensures that the analytes take on negative charges resulting in less analyte-wall interaction and thus reducing band broadening. All these factors namely: - capillary diameter, choice of buffer and electrophoresis pH have to be optimized. [42]

Use of nanoparticles in capillary electrophoresis

Modification of gold nanoparticles

Nanobiotechnology has attracted immense attention in the fields of chemistry, physics and biology. The application of nanomaterials is rapidly rising and is shaping the science of separation. Due to their large surface area to volume ratio, nanoparticles have the ability to selectively interact with the capillary surface, the analyte or both

culminating into high mass transfers and dramatically changing the parameters of a separation.[23]

These small particles have a large surface area to volume ratio, a characteristic that can be successfully exploited in capillary electrophoresis. The large surface area can act as a platform for the adsorption of ligands that interact differentially with the analytes, offering another mode of separation. Taken together, these attributes offer a tremendous increase in the precision and separation efficiency of CE as a technique.[18,23]

The use of nanoparticles in CEC has attracted a great interest and was recently reviewed by Guihen and Glennon. Different materials have been utilized for the production of nanoparticles including gold, silver, silica, fullerene and organic polymers. Different ligands have previously been attached onto the surface of nanoparticles to increase the selectivity with which they interact with specific analytes. The surface modification of nanoparticles offers several major advantages to capillary electrochromatography, namely: - it prevents the aggregation of the nanoparticles and ensures even dispersion when in solution, it controls the particle size, and the functional groups on the chemisorbed molecules interact differently with specific analytes offering an extra level of selectivity during separation.[24]

Bare or modified gold nanoparticles have been used to increase the efficiency, specificity and reproducibility of CE separations. Studies done by Pumera *et al.* show that the efficiency of separations in microchip capillary electrophoresis can be greatly improved by the use of nanoparticles. In their study, citrate stabilized gold nanoparticles (10 nm diameter) were used to improve separation of aminophenols. They reported that

the resolution and plate numbers of the solutes doubled compared to conventional bare silica capillary electrophoresis. This was attributed to the changes of electrophoretic and electroosmotic mobility of solutes in the presence of gold nanoparticles.[25]

Yu *et al.* used gold nanoparticles modified with polyethylene oxide in the separation of double stranded DNA, achieving an efficiency of 10^6 plates/M. Didodecyldimethylammoniun bromide bilayer protected 6 nm diameter gold nanoparticles were also used to effectively separate acidic and basic proteins and reduced peak migration deviations by 0.6% compared to normal CE.[26] Glennon *et al.* pre-derivatized fused silica capillaries with dodecanethiol modified gold nanoparticles for the separation of drug compounds.[27]

The nanoparticles are used as a pseudo stationary phase that offers a large surface area for interaction with analytes while occupying a small volume. These nanomaterials can either be introduced into the capillary prior to the analytes (partial filling) or continuously introduced into the capillary throughout the process of separation whilst having uniform mobility and not tampering with detection capabilities of the technique. A great challenge in the use of nanoparticles is the tendency to form small clusters a process commonly known as aggregation. For efficient separation, it is necessary to maintain the nanoparticles in a stable suspension while in aqueous solutions during the process of separation. This is mainly done by covalently modifying the nanoparticles.[18]

According to Gottlicher and Bachmann the ideal nanoparticles should have the characteristics outlined below: - (i) be charged during separation in order for them not to co-elute with EOF. (ii) form stable suspensions in solution and be able to selectively

interact with different analytes in order to create a difference in migration time and have the power of separating neutral analytes. (iii) exercise equal mobility during electrophoresis to avoid band broadening. (iv) have a large surface area to volume ratio (v) have the least possible mass transfer resistance and should not interfere with detection of analytes.[21]

The biggest drawback of pseudo stationary phase – capillary electrochromatography (PSP-CEC) is the interference by the nanoparticles during detection by UV due to their light scattering properties. This can however be avoided by the use of a laser induced fluorescence detector that filters out Rayleigh scattering. The analytes are first derivatized with fluorescent molecules prior to separation. For detection, a laser is used to excite the analyte- fluorophore complex and the signal thereby obtained is integrated as a measure of the concentration of analyte. [18,32]

Self assembled monolayers

Derivatization of gold nanoparticles used in capillary electrochromatography as a pseudo stationary phase is done by the creation of self assembled monolayers (SAMs) on the surface of the gold nanoparticles. SAMs are organic assemblies formed onto a solid surface from solution by chemisorption. There are two main forces that play a role in the chemisorption of thiol containing ligands onto gold metal surfaces. (i) The affinity of sulfur for the gold surface. The sulfur-gold bond is in the order of 45 kcal/mol which is a stable semi-covalent bond. This is fairly strong considering that the C-C bond strength is about 83 kcal/mol. (ii) The methylene carbons on the carbon chains exhibit Van der

Waals interactions. These interactions make the carbon chains tilt in their positions in order to lower the overall surface energy. Initially, the monolayer formed contains many gauche defects, but the alkyl chains become more ordered over time (12-18 hours) to form a closely packed monolayer as shown by the Figure 4. Research has shown that the best ordered monolayers are derived from alkyl chains that are about 10 carbons long.[35, 36, 37]

Optical properties of gold nanoparticles depend on the core size of the particles in solution. Small particles of less than 3 nm exhibit a surface plasmon resonance maxima around 200 nm range while larger particles > 3 nm have a characteristic surface plasmon resonance at around 520 nm. The particles therefore appear to have a red color that can be used for their characterization.[37]

Figure 4. Chemisorption of thiols onto a gold surface

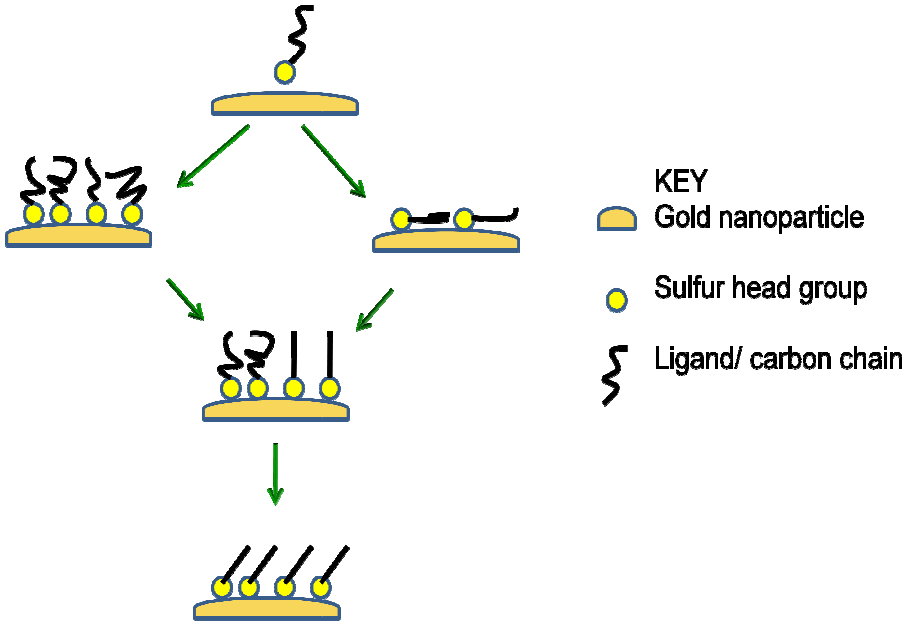

The carbon chains become more ordered over time as the alkyl chains tilt for maximum interaction among the methylene groups.

The use of neutral thiols for derivatization of citrate stabilized nanoparticles is discouraged because it leads to nanoparticle aggregation evidenced by a color change of the solution from red to blue due to a red shift of surface plasmon bands. Nanoparticles coated with self assembled monolayers having a mercaptoundecanoic acid head groups are more stable because the deprotonated carboxylic acid group provides electrostatic stability to the colloid which prevents nanoparticle aggregation.[38]

Self assembled monolayers on gold can easily be created by chemisorbed molecules with disulfide or thiol groups. Dialkyl disulfides and alkanethiols have been utilized in the creation of monolayer protected clusters (MPC) on gold nanoparticles. Young *et al.* studied the composition of monolayers on gold nanoparticles formed from asymmetric disulfides $CH_3(CH_2)_{11}S\text{-}S(CH_2)_{11}OH$ and symmetrical disulfide $CH_3(CH_2)_{11}S\text{-}S(CH_2)_{11}CH_3$. The derivatized gold nanoparticles were then characterized by UV spectroscopy, NMR spectroscopy, Infrared spectroscopy and Transmission Electron Micrographs.[28]

Creation of ordered monolayers on metal surfaces requires the use of surface terminating groups such as $-NH_2$, -SH or -CN, that enable the spontaneous adsorption. -SH terminated molecules have found wide application in these Self Assembled Monolayers (SAMs) due to their high stability. Thomas *et al.* modified gold nanoparticles with 1-dodecanethiol and probed their ability to discriminate between benzophenone and biphenyl solutes in a capillary electrochromatography (CEC) separation with a total separation time of less than five minutes. [29]

Self assembled monolayers can effectively be made from thiols or disulfides. Studies of SAMs made from asymmetric disulfides ($RSSR^1$) have shown that both halves of the disulfide -S-R and $–S\text{-}R^1$ are incorporated into the SAMs in a 1:1 ratio. This supports the hypothesis that thiols and disulfides react at the gold surface forming thiolate intermediates. The sulfur-sulfur bond of the disulfide is cleaved yielding the two possible thiolate species. The thiolates then act independently to chemisorb onto the gold surface to form a new gold-thiolate species. It was also shown that longer chain thiols are capable

of displacing shorter chain thiols from an already formed monolayer. The affinity of gold for sulfur and the lack of a surface oxide on gold are exploited in the assembly of monolayers through covalent interactions with sulfur groups and therefore, it is easier to derivatize gold nanoparticles compared to silica or silver nanoparticles.[30]

Factors that affect the formation of self assembled monolayers.

Several aspects have to be considered during the procedure for the derivatization of gold nanoparticles. Among the conditions that are known to have an effect on the formation of self assembled monolayers include: - temperature, concentration and reaction time of the chemisorbing species, solvent used, purity of disulfide or thiol and substrate (gold).

Temperature

Reaction temperatures above 25 °C have been shown to favor the reaction kinetics of monolayer formation and reduction of defects in the formed ligands. These elevated temperatures help in the desorption of solvent molecules that are in association with the substrate surface and any other substances used for the stabilization of the colloidal gold. This temperature elevation also helps in overcoming of the activation barrier and adsorption of the ligands onto the gold nanoparticles. Since the adsorption of ligands is spontaneous and occurs in the order of milliseconds to minutes, the slightly elevated temperatures (50 °C) were found to be important in the initial process of derivatization.[39,40]

Concentration of chemisorbing species and reaction time

The lower the concentration of chemisorbing species, the longer the time required to form a well ordered monolayer on the substrate. The typical maximum coverage for self assembled monolayers is approximately 4.5×10^{14} molecules/cm^2 and therefore the minimum concentration for forming a good SAM is about 1 µM which corresponds to 6 $\times 10^{14}$ molecules/cm^3. Dense monolayers can be assembled in a matter of milliseconds to minutes using milimolar concentrations of the chemisorbing species. For long chain thiols, the immersion of the substrate in a 1 µM solution containing chemisorbing species for periods of 12-18 hours is sufficient to form a dense monolayer, indistinguishable from that formed from higher concentrations. Longer immersions in the order of days can however greatly decrease the number of pinhole defects and improve the order of the alkane chains. This helps in the improvement of the reproducibility of experiments for which the SAMs are used. [41]

Solvent

Several solvent systems including ethanol, tetrahydrofuran, dimethylformamide, acetonitrile, cyclooctane and toluene have been used for the preparation of SAMs, however, ethanol has been widely used because it easily solvates thiols and disulfides of different chain lengths, it is inexpensive, is available at high purity and is non toxic. Bain *et al.* found that SAMs formed in ethanolic solutions did not vary significantly from those made using other solvents.[35]

Characterization of derivatized gold nanoparticles

Surface plasmons are the fluctuations of electron density at the boundary of two materials. The excitation of surface plasmons is called surface plasmon resonance (SPR). This characteristic can be used for the monitoring of adsorption of materials onto the surface of metal nanoparticles. The SPR extinction spectrum band is determined by the size, shape and the refractive index around the surface of the gold nanoparticles. The inter-particle distance also plays a major role in the type of spectrum obtained.[46]

A beam of light consisting of visible or infra-red frequencies can be used to excite the surface plasmons. This incident light can either be reflected of refracted. Above a critical angle of incidence, no refracted light is observed, instead a total internal reflection is observed. During the creation of self assembled monolayers, the chemisorbed layer induces a local refractive index change around the surface of the gold nanoparticles. This change can easily be monitored by either scattering of absorption techniques. The apparent increase in refractive index is accompanied by a red shift of the surface plasmon band.[47]

Jin *et al.* observed a red shift in the surface plasmon band of gold nanoparticle capped with dodecanethiol when compared to non derivatized gold nanoparticles. They also noted that the thicker the self assembled layer, the more the surface plasmon band was observed towards longer wavelength. Gold nanoparticles derivatized with the highest amount of dodecanethiol exhibited the most red shifted SPR. They attributed the red shift of SPR to the increasing size of the nanoparticles caused by the increase in amount of dodecanethiol.[48]

Numerous studies have been done on the separation and analysis of Alzheimer's disease biomarkers using capillary electrophoresis with an aim of improving the disease diagnosis and progression monitoring. Gold nanoprticles have been used in improving the separation of different peptides when used as a pseudo stationary phase in capillary electrochromatography. Derivatization of the gold nanoparticles with different alkyl branches could allow a differential interaction between different analytes and the gold particles during electrophoresis, leading to an improved separation of the analytes. An asymmetrical disulfide was synthesized and used to derivatize gold nanoparticles. The particles were eventually used in capillary eletrochromatography analysis of Alzheimer's disease biomarkers.

CHAPTER III

SYNTHESIS AND CHARACTERIZATION OF ASYMMETRIC DISULFIDE

Introduction

In order to produce a pseudo stationary phase that could interact with Alzheimer's disease biomarkers differently, an asymmetric disulfide with a long alkyl chain (12 C) and a carboxylic acid chain (11 C) as shown below was synthesized.

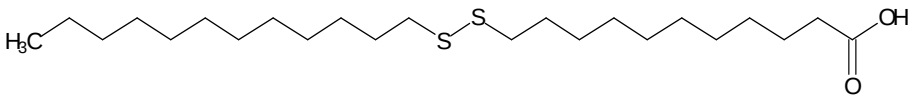

Asymmetric disulfides can easily be synthesized by a coupling reaction of two thiols, however, this direct reaction is prone to many side reactions some of which lead to the formation of the symmetrical disulfides.[38, 39, 40] The carboxylic acid functional group further complicates the reaction since the carbonyl can act as an electrophilic site triggering substitution of the hydroxyl group in side reactions. It was therefore important to protect the carboxylic acid group first before coupling the two thiols. This protection was accomplished by esterification of the carboxylic acid using ethanol. The synthesis scheme in Figure 5 was used.

Figure 5. Synthesis scheme of asymmetric disulfide

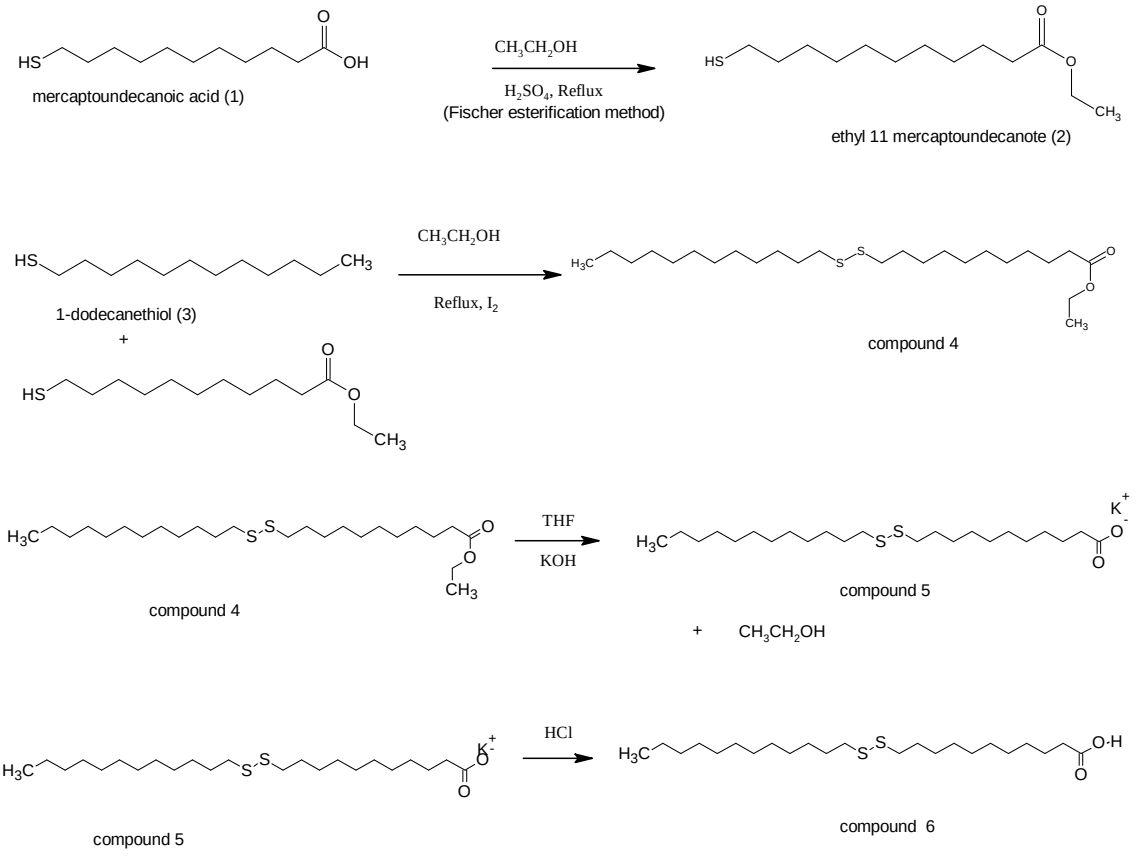

Materials and methods

Iodine, dichloromethane, ammonium hydroxide, hydrochloric acid, sulfuric acid, sodium metabisulfite, magnesium sulfate and sodium bicarbonate were all obtained from Fisher Scientific. Hexane, tetrahydrofuran, potassium hydroxide, deuterated chloroform and 11-mercaptoundecanoic acid were purchased from Aldrich, 1-dodecanethiol and 60-

100 mesh silica (Florisilr) were from Acros Organics, absolute ethanol (200 proof) from Pharmco Aaper Alcohol & Chemical Co. Gold nanoparticles were purchased from Sigma and BBInternational.

Procedure for synthesis of asymmetric disulfide

Preparation of Ethyl-11-mercaptoundecanoate $HS(CH_2)_{10}COOCH_2CH_3$

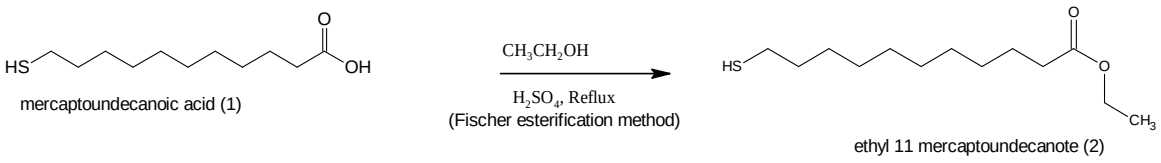

Ethyl-11-mercaptoundecanoate was prepared from mercaptoundecanoic acid and ethanol by the Fischer esterification method. 5.00 g of 11 mercaptundecanoic acid (mwt 218.36, 0.0229 moles) were dissolved in 140 mL of absolute ethanol in a 250 mL round bottom flask then 3 drops of concentrated H_2SO_4 were added. The flask was fitted with a condenser and the mixture was heated with stirring and refluxed for 16 hours. The reaction was closely followed by Thin Layer Chromatography (Baker-flex Silica gel IB2-F). Once the starting material was no longer visible on thin layer chromatography, heating was stopped and the reaction mixture was allowed to cool to room temperature. The ethanol was removed under reduced pressure and the reaction mixture re-dissolved in 50 mL of dichloromethane. The mixture was washed thrice with 50 mL volumes of saturated sodium bicarbonate in order to get rid of the sulfuric acid. The dichloromethane

layer was dried over anhydrous magnesium sulfate and rotary evaporated to give 5.2 g of ethyl-11- mercaptoundecanoate. This was a yield of 92%.

Synthesis of compound 4

5.2 g of ethyl-11-mercaptoundecanoate (mwt 262.4 g, 0.0198 moles) and 4.00 g of 1-dodecanethiol (mwt 202.40 g, 0.0198 moles) were dissolved in 100 mL of ethanol in a 500 mL round bottom flask. Iodine was added into the reaction mixture until the mixture turned a constant brown color. The mixture was refluxed at 78 °C for a period of 16 hours. The reaction was monitored by thin layer chromatography (TLC).

The ethanol was evaporated under reduced pressure out of the reaction mixture leaving behind a black residue which was then dissolved in 50 mL of dichloromethane. This solution was washed thrice with concentrated sodium metabisulfite ($Na_2S_2O_5$) to remove iodine from solution. The brown color of iodine disappeared and two clear layers of sodium metabisulfite and dichloromethane formed.

The dichloromethane layer was dried over magnesium sulfate, filtered and rotary evaporated under reduced presure to 8.72 g of a white solid (compound 5, mwt 463.80 g, 0.188 moles). The compound was further purified using column chromatography. A 2 cm diameter column was packed with silica gel (60-100 mesh) and equilibrated using hexane. 0.5 mL of the reaction mixture was separated at a time. Elution was first done with 100 mL of 100% hexane then a gradient worked up to 100% dichloromethane. Fractions with similar compounds were combined and solvents evaporated under reduced pressure. Both compounds were white solids at room temperature. Nuclear Magnetic

Resonance Spectroscopy was performed to identify compound 4 (R_f = 0.40 on TLC) which had a yield of 8.51 g (97%).

Synthesis of compound 5 and 6

The 8.51 g (0.018 moles) of compound 4 was dissolved in 100 mL of tetrahydrofuran (THF), 3.02 g of potassium hydroxide (KOH) (mwt 56.088 g, 0.054 moles) was dissolved in 20 mL of 1:1 mixture of H_2O/C_2H_5OH. This reaction mixture was stirred for 12 hours at room temperature while being monitored by TLC. Once the starting materials had disappeared, the mixture was acidified with 20 mL of 2 M HCl. The mixture was cooled in an ice bath and white crystals formed out of solution. The crystals were washed with cold THF and water then dried under *vacuo*. 8.3 g of compound 6 were obtained.

Proton NMR

Proton NMR (^{1}H NMR) spectra were all obtained using a JEOL ECA 500 MHz spectrometer by dissolving 10 mg of the compound of interest in 0.5 mL of deuterated chloroform ($CDCl_3$). The data obtained was integrated using the DELTA software.

Results

^{1}H NMR samples were prepared by dissolving 10 mg/mL of the compound of interest in 0.5 mL of deuterated chloroform ($CDCl_3$), unless otherwise stated.
The data obtained was integrated using the DELTA software.

Figure 6. ^{1}H NMR of ethyl-11-mercaptoundecanoate

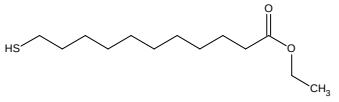

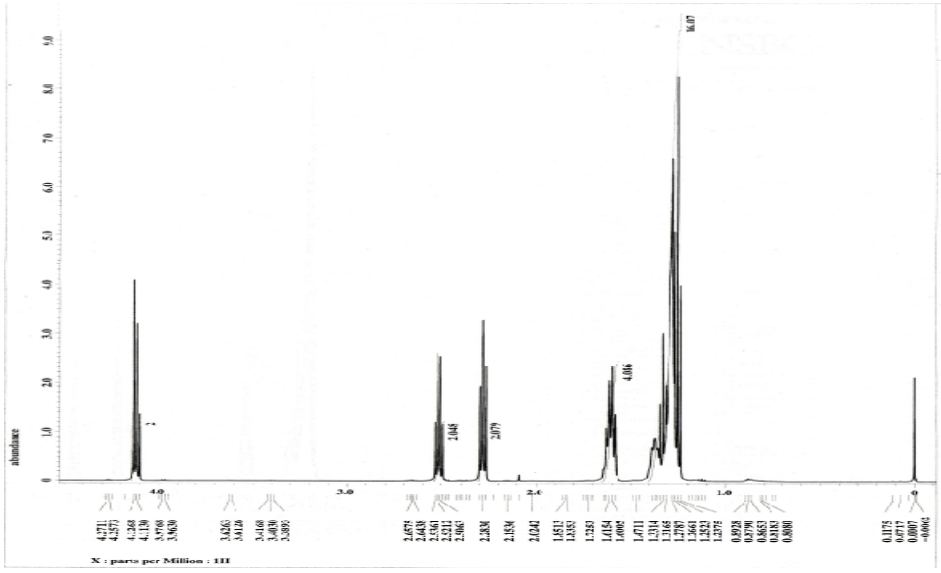

^{1}H NMR ($CDCL_3$, TMS) δ 1.23-1.33 (m, 16H, -C***H***$_3$, -S***H***, $HSCH_2CH_2$-(C***H***$_2)_6$-), 1.58-1.63 (m, 4H, $HSCH_2$-C***H***$_2$-, C***H***$_2CH_2COO$-CH_2CH_3), 2.28 (t, 2H, -C***H***$_2COO$-CH_2CH_3), 2.52(q, 2H, HS- C***H***$_2$-), 4.12 (q, 2H, -CH_2COO-C***H***$_2CH_3$).

Figure 7. ^{1}H NMR of compound 4

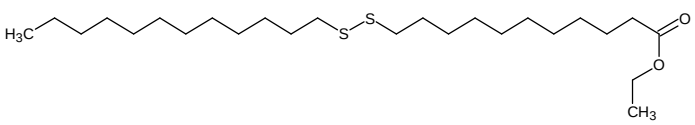

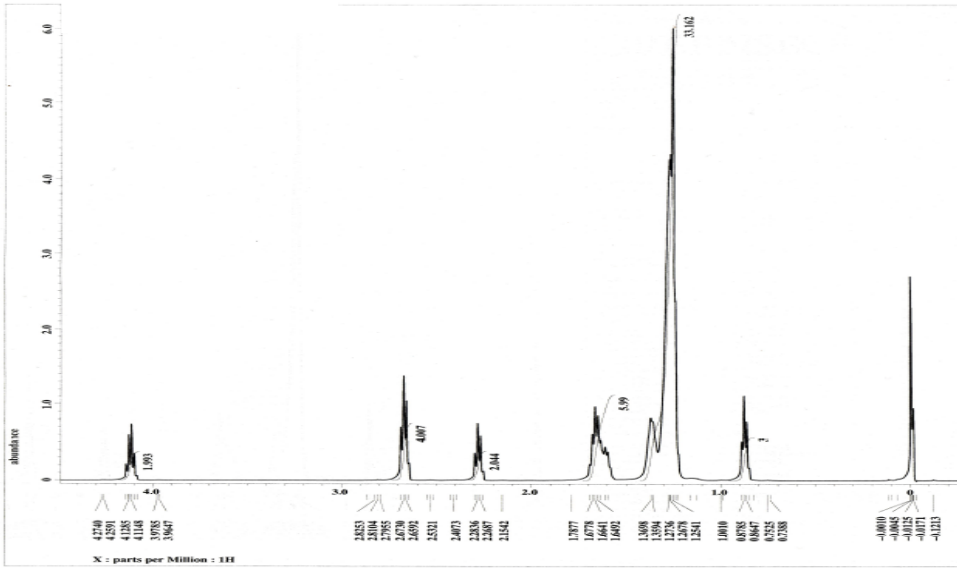

^{1}H NMR ($CDCl_3$, TMS) δ 0.88 (t 3H, -C***H***$_3$), 1.20-1.46 (m, 33H, - COO-CH_2-C***H***$_3$ - SCH_2CH_2-(C***H***$_2$)$_9$-CH_3, -SCH_2CH_2(C***H***$_2$)$_6$$CH_2CH_2$COO-), 1.58-1.74 (m, 6H, -SCH_2-C***H***$_2$-, -C***H***$_2$-CH_2CO_2-), 2.28 (t, 2H, -C***H***$_2$-$CO_2CH_2CH_3$), 2.66 (t 4H, S-S-C***H***$_2$-CH_2-), 4.12 (q, 2H, - COO-C***H***$_2$-CH_3).

Figure 8. ^{1}H NMR of the desired asymmetric disulfide (compound 6)

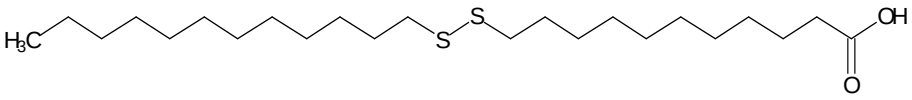

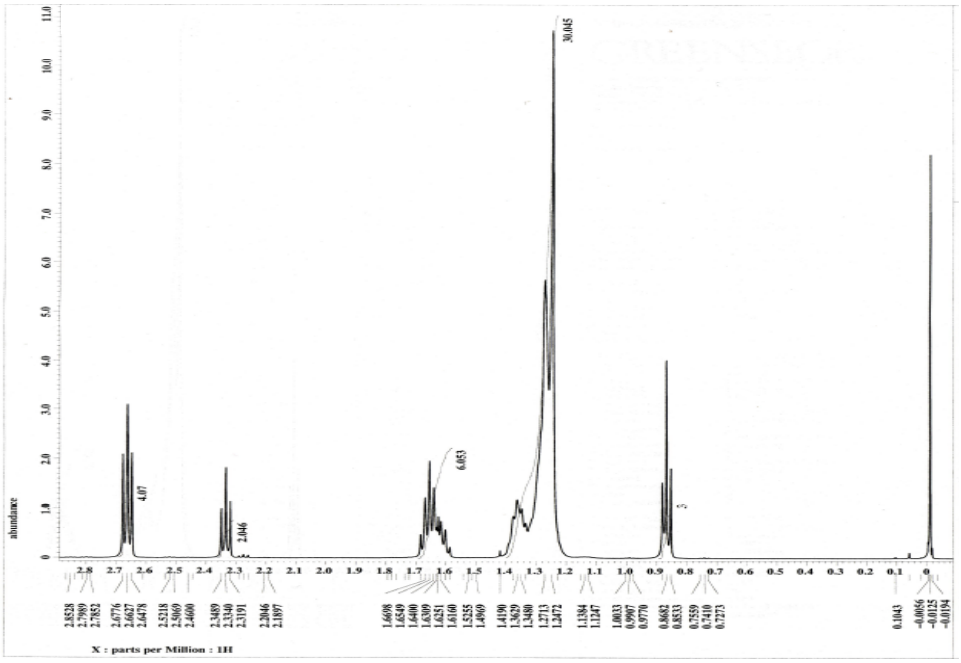

1H NMR ($CDCl_3$, TMS) δ 0.87 (t, 3H, -C***H***$_3$), 1.20-1.44 (m, 30H, -SCH_2CH_2-(C***H***$_2$)$_9$-CH_3, -SCH_2CH_2(C***H***$_2$)$_6CH_2CH_2COOH$), 1.58-1.74 (m, 6H, -C***H***$_2$-CH_2-S-S-CH_2-C***H***$_2$-, -C***H***$_2$-CH_2CO_2), 2.33 (t, 2H, -C***H***$_2$-CO_2), 2.66 (t, 4H, -S-S-C***H***$_2$-CH_2-).

^{13}C NMR of asymmetric disulfide (compound 6)

The COOH proton has a characteristic absorbance between δ 10 and δ 12 which is generally weak; however, the presence of a carboxylic acid group can easily be confirmed by analysis of the compound by ^{13}C NMR. This is evidenced by the strong absorbance around δ 180. Figure 9 shows an NMR spectra of the final disulfide at a concentration of 50 mg/mL in deuterated chloroform ($CDCl_3$).

Figure 9. ^{13}C NMR of asymmetric disulfide (compound 6)

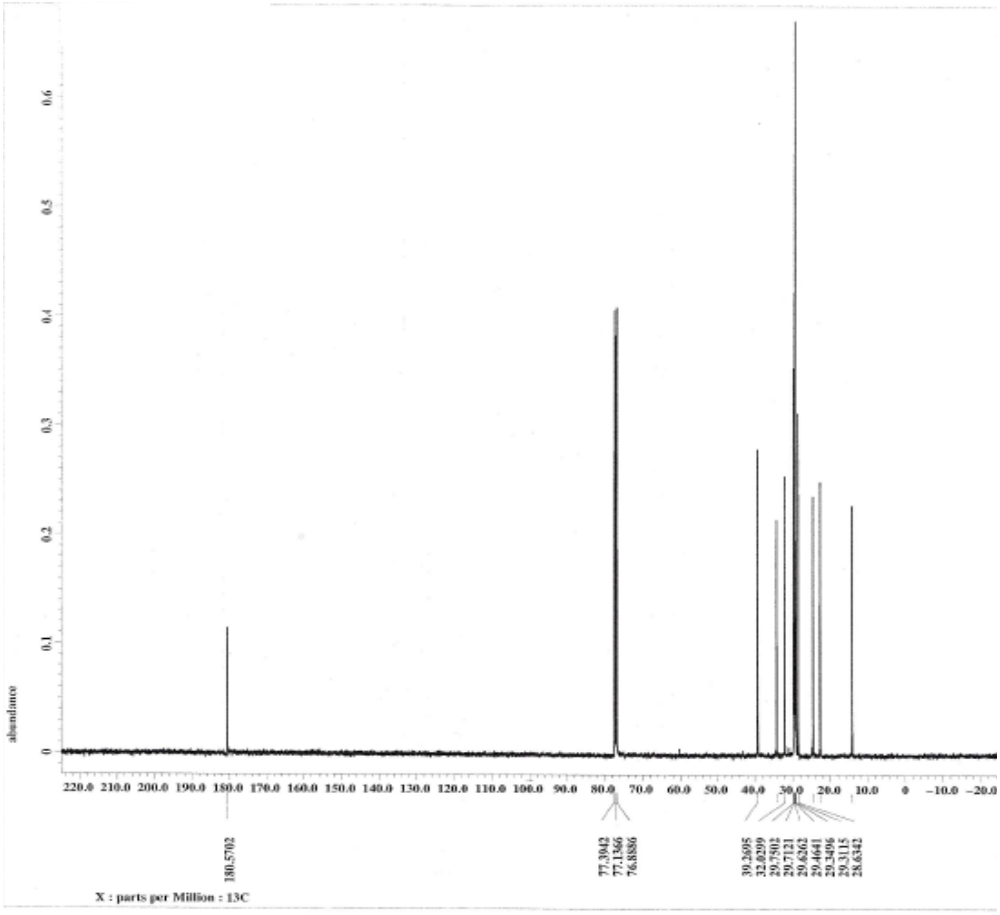

The peak at δ 180.57 in figure 9 is representative of the C in the COOH group. This further confirmed the identity of the disulfide. Having been well characterized, the disulfide was then used for modification of gold nanoparticles. Structural and compositional analysis of the modified nanoparticles was performed using UV spectroscopy.

CHAPTER IV

DERIVATIZATION AND CHARACTERIZATION OF GOLD NANOPARTICLES

Introduction

The goal was to create gold nanoparticles with a monolayer on them consisting of 1:1 ratio of mercaptoundecanoic acid and dodecanethiol ligands, hence the name mixed self assembled monolayers. This assembly was accomplished by chemisorption of an asymmetric alkyl disulfide synthesized from dodecanethiol and mercaptoundecanoic acid (MUA) onto citrate stabilized gold nanoparticles with an average diameter of 10 nm.

The choice of MUA and dodecanethiol as the ligands making the monolayer was made with an idea of maximizing the interaction between the synthesized nanoparticles and AD biomarkers. The alkyl chain from dodecanethiol offers hydrophobic interactions while carboxylic acid chain has three major functions; it offers hydrophilic interactions with the biomarkers, has a negative charge that creates electrostatic stability to minimize aggregation of nanopaticles and ensures that the particles experience an electrophoretic force in the presence of an electric field due to its negative charge.

Derivatization of the nanoparticles with the asymmetric disulfide enabled stability of the monolayers in a wide range of pH and in different aqueous solutions and buffers. Separations were performed at pH ranges above 4.6 where the carboxylic acid chain is deprotonated.

Due to the high negative charge density, the particles when suspended in the buffer “migrate” towards the anode caused by their electrophoretic mobility. The migration of AD biomarkers in the electric field offers substantial interactions with the gold nanoparticles, however, since electroosmotic flow is greater than electrophoretic mobility, net movement is towards the cathode. The more a biomarker interacted with the nanoparticles, the higher its retention time, hence an inverse relationship of migration time and interaction was observed as illustrated in Figure 10.

Figure 10. Gold nanoparticles in capillary electrochromatography

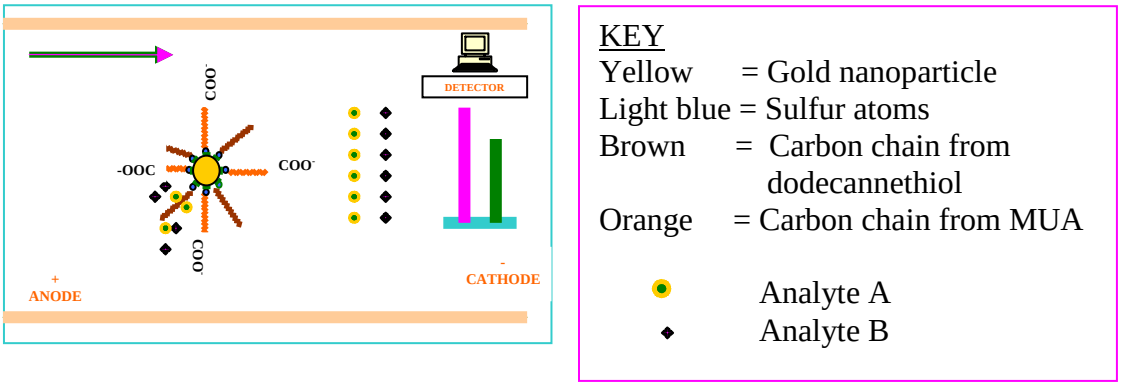

Analyte A has stronger hydrophobic interaction with the alkyl chains chemisorbed onto the gold nanaoparticle and thus spends more time in the capillary as opposed to analyte B which has a lesser interaction. Analyte A therefore arrives at the detector after

B as seen by the peaks from the detector. The arrow in the diagram shows the general direction of flow.

Materials and methods

The non derivatized gold nanoparticles were stored at 4 ℃ to maintain stability. 2.0 mL of citrate stabilized gold nanoparticles were obtained from the refrigerator and allowed to warm up to room temperature for 20 minutes; they were then immersed into a water bath until a constant temperature of 50 ℃ was reached. 5 mL stock solution of 1 millimolar disulfide solution was prepared by dissolving 2.085 mg of asymmetric disulfide in tetrahydrofuran. 1 mL of the disulfide solution was warmed to 50 ℃ in a water bath. 100 µL of the warm disulfide solution was drawn and slowly mixed with the gold colloid and thoroughly stirred at room temperature.

After 12 hours, the reaction mixture was centrifuged at 10,000 g for 30 minutes and the supernatant decanted, leaving behind a pellet of derivatized gold nanoparticles. The derivatized nanoparticles were washed twice with 500 µL of 1:1 mixture of tetrahydrofuran: nanopure water, followed by centrifugation each time and decantation of the supernatant. The derivatized gold nanoparticles were then re-dissolved into 2 mL of running buffer and used as a pseudo stationary phase for analysis of amyloid beta peptides in a capillary electrophoresis – laser induced fluorescence instrument. Derivatization of gold nanoparticles was monitored using a CARY 100 Bio UV-Visible spectrophotometer from Varian. The concentration is ~ 5.7×10^{12} particles of gold

nanoparticles/cm^3 of solution, which is the concentration of the gold nanoparticles as given by the manufacturer.

Results and discussion

The particles were mixed with the asymmetric disulfide as explained in materials and methods then monitored for a period of 3 days.

Figure 11. UV-Vis Spectroscopy results of the continuous derivatization of 10 nm gold nanoparticles

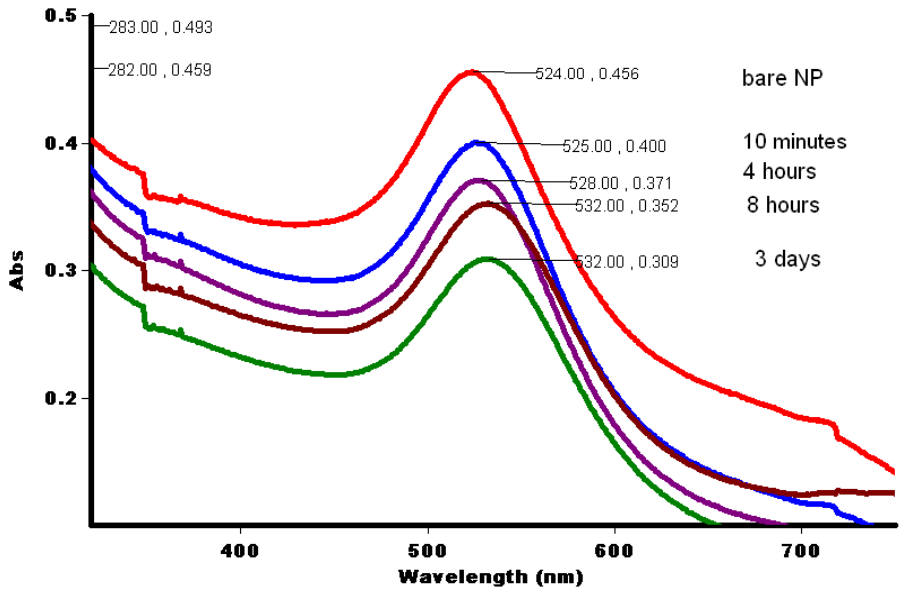

Table 1. Derivatization time versus surface plasmon maxima of gold nanoparticles

Derivatization time	Surface Plasmon band (nm)
2	524
10 Minutes	525
4 hrs	528
8 hrs	532
3 days	532

UV-Visible measurements were done before, during and after the process of derivatization. Initial surface plasmon band of citrate stabilized gold nanoparticles was observed at λ_{max} 520 nm which is an intrinsic characteristic of 10 nm diameter gold nanoparticles. A red shift to 525 nm of the plasmon peak was observed immediately after mixing the particles with 1 mM disulfide, this change was attributed to the changes occurring in the local dielectric constant around the gold nanoparticles due to the chemisorption of ligand monolayers on the gold surface. This shift towards longer wavelength continued to occur with time and was shown to stabilize at 532 nm after a period of 8 hours.

Figure 12. UV spectra of derivatized versus non derivatized gold nanoparticles

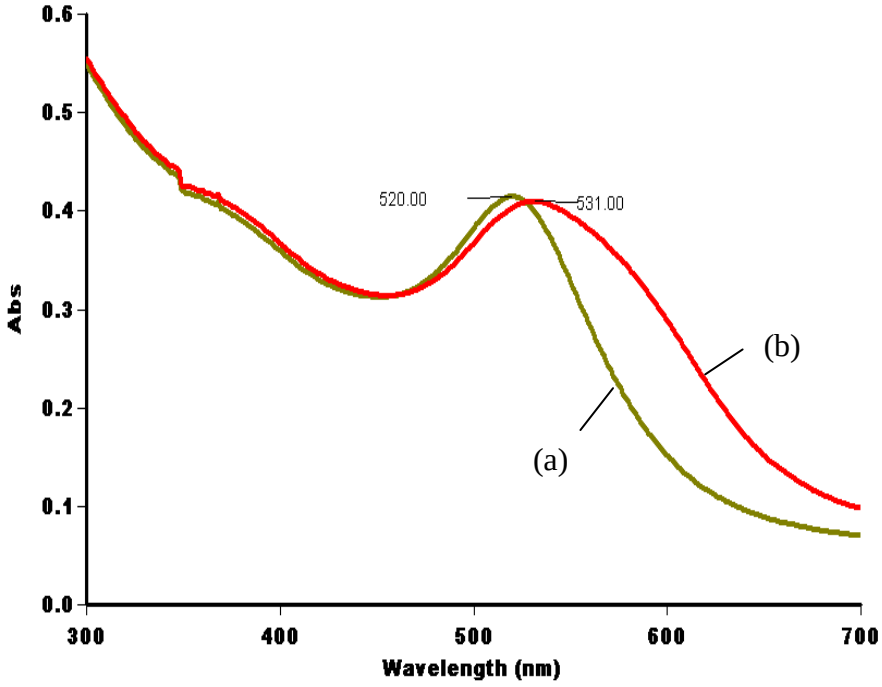

Trace (a) with a maximum surface plasmon resonance of 520.00 nm and relative intensity of 0.414 units represents non derivatized gold nanoparticles as received from the supplier while trace (b) with maximum surface plasmon resonance of 531.00 nm and relative intensity of 0.409 units represents gold nanoparticles derivatized for 8 hours without any centrifugation or washing.

The characteristic maximum surface plasmon resonance of 10 nm gold nanoparticles at 520 nm is clearly seen on the green trace. A shift in surface plasmon resonance of 11 nm towards longer wavelength between the non derivatized and

derivatized form of the gold nanoparticles can be attributed to the formation of a self assembled monolayer on the surface of the gold nanoparticles. The nanoparticles in both cases (non derivatized and derivatized) were centrifuged and washed as outlined in materials and methods and their UV spectrum taken to give the results in Figure 13.

Figure 13. UV spectra of derivatized and non derivatized gold nanoparticles(washed)

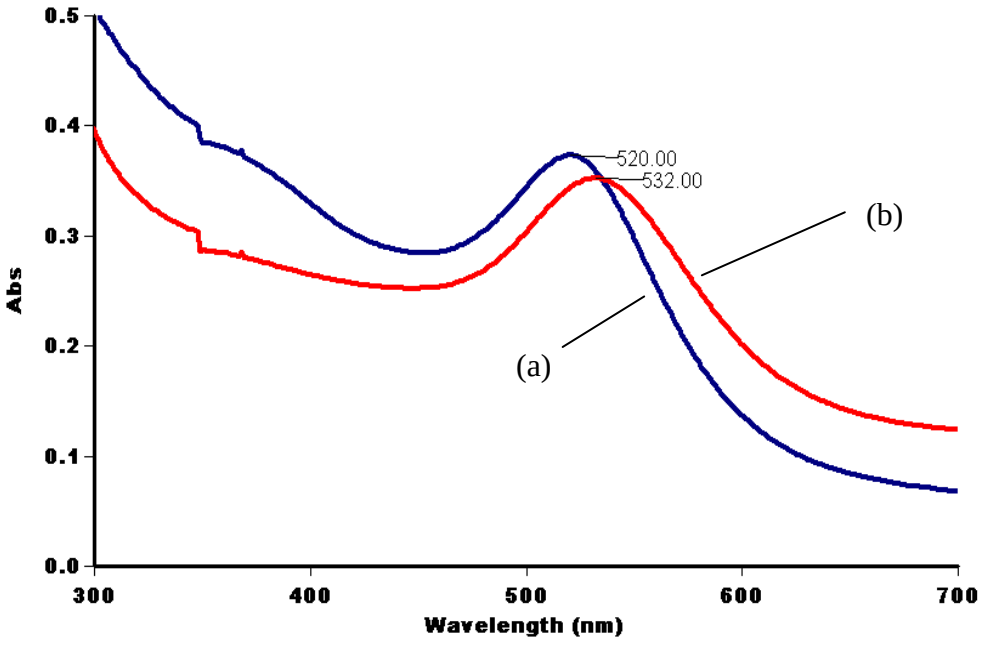

The blue trace (a) with a maximum surface plasmon resonance of 520 nm and a relative intensity of 0.373 units represents non derivatized gold nanoparticles while the red trace (b) with a maximum surface plasmon resonance of 532 nm and a relative

intensity of 0.352 units represents the derivatized form. Both samples were washed and re-dissolved in nanopure water as explained in materials and methods, the only difference being that the sample represented by the red trace had been derivatized. The surface plasmon resonance for the derivatized form of the gold nanoparticles shifts insignificantly to a longer wavelength by 1 nm compared to surface plasmon resonance maximum of 531 nm before washing, while that of the non derivatized form remains at 520 nm.

The intensities of surface plasmon resonance after washing are however reduced to 0.373 and 0.352 down from 0.414 and 0.409 units for the non derivatized and derivatized forms respectively. This decrease was attributed to the fact that not all the nanoparticles were able to be sedimented during centrifugation, a factor which was also evidenced by the faint reddish color of the centrifugation supernatants. The resulting gold nanoparticle solutions had slightly fewer particles than the original amount hence the reduced surface plasmon resonance intensity.

Conclusion

Derivatization of the gold nanoparticles was done overnight at room temperature. It was observed that the color of gold nanoparticles remained light-red and well dispersed in solution even after the centrifugation and washing procedures were performed. No reduction in surface plasmon resonance intensity indicative of nanoparticle aggregation was observed for at least 3 days. Aggregation is mainly evidenced by band broadening and diminishing surface plasmon resonance peak intensity. [37] None of these

characteristics were observed in the derivatized nanoparticles. The derivatized nanoparticles were found to be colloidally stable for more than 3 days.

CHAPTER V

ANALYSIS OF ALZHEIMER'S DISEASE BIOMARKERS USING CAPILLARY ELECTROCHROMATOGRAPHY

Introduction

Electrophoresis is the differential migration of ions by attraction or repulsion in an electric field. CE is based on the differential migration of charged species through a silica capillary. The ends of the capillary are placed in buffer reservoirs with electrodes which are connected to a source of high voltage. Samples are introduced into the capillary usually at the anodic end either electrokinetically or hydrodynamically. High voltage is then applied across the capillary to perform the separation. The migration of analytes is caused by electroosmotic flow (EOF) and electrophoretic flow in the presence of a separation buffer. Detection can be done online or off-line at the cathodic end.

Typically, capillaries of 50-100 µm internal diameters are used; although smaller and larger capillaries are commercially available. The ends of the capillary are placed in buffer reservoirs that have electrodes which are connected to a source of high voltage. Samples are introduced into the capillary usually at the anodic end either electrokinetically or hydrodynamically. High voltage is then applied across the capillary to perform the separation. After the separation, detection can be done online or off-line at the cathodic end.

Amyloid beta peptides were derivatized with ATTO-TAG FQ^{TM}, a fluorogenic compound to make the peptides fluorescent and diluted as specified in each experiment. Hydrodynamic injections were done at the capillary inlet followed by application of electrophoresis voltage. Detection was performed using a laser-induced fluorescent detector near the end of the capillary.

Materials and methods

Preparation of fused silica capillaries

Fused silica capillaries of inner diameter 50 µm and outer diameter of 361 µm were used in all experiments. A detection window was made 50 cm from inlet to detector. The geometry of the capillary end at the inlet is important due to the interaction of the capillary and the surface of the liquid during and after sample injection. A rugged surface can cause expulsion of injected sample plug, leading to inconsistencies in reproducibility. The polyimide coating of the capillary was therefore burned off at both ends to remove the rugged surface.

Electroosmotic flow in CE is due to the silanol groups found on the inside surface of the capillary, these groups are enhanced by running a basic solution through the capillary before its first use, a step commonly known as “conditioning”, the base increases the concentration of the silanol groups. Fused silica capillaries were conditioned by flushing them with 1M sodium hydroxide for 10 minutes before their first use in separation, this conditioning step creates silanol groups which form a layer at the silica–liquid interface responsible for the building up of an electrical double layer during

separation. This was followed by a 10 minute flush with 0.1 M sodium hydroxide solution then a 10 minute flush with nanopure water. The capillary was then ready for use in separation experiments.

At the beginning of the every analysis, the capillary was regenerated and reconditioned by washing it with sodium hydroxide (0.1 M) for 5 minutes, nanopure water for 5 minutes, and finally, running buffer for 5 minutes. Sodium hydroxide etches fused silica and therefore it is well suited for washing off the capillary column. This action ensured that any analyte remnants from previous analyses were washed out of the column to avoid contamination.

Dissolution and storage of peptide samples and derivatization reagent

The medium in which amyloid beta peptides are dissolved is critical since the peptides tend to aggregate under certain conditions of pH and temperature. Aβ 42 and Aβ 40 were separately dissolved in 1% ammonium hydroxide as suggested by the supplier to a final concentration of 1.25×10^{-4} M. The stock solution was divided into aliquots of 4µL each in 500 µL micro-centrifuge tubes and stored in a refrigerator at a temperature of -20 °C. Samples were thawed only once before analysis. 10 mM solution of the derivatization reagent ATTO-TAG FQ™ (3-(2-furoyl) quinoline-2-carboxaldehyde 2) was prepared by dissolving 10 mg of the derivatizing agent into 4 mL of 99.9% methanol. Aliquots containing 100 nM of ATTO-TAG FQ™ were transferred into 500 µL micro-centrifuge tubes and the methanol removed by rotary evaporation under vacuum at room temperature before storage at -20 °C.

Preparation of separation buffer, sodium hydroxide and potassium cyanide

Borate buffer was used for initial studies. 100 mM stock solution was prepared and filtered through 0.45 µm Whatman nylon membrane filters. Fresh working buffers were made daily from the stock solution by dilutions with nanopure water and adjusting the pH to a desired value using 0.1 M HCl or 0.1 M NaOH. 10 mM potassium cyanide was made by dissolving 6.5 mg of KCN in 10 mL of 10 mM running buffer at pH 10. In all cases nanopure water was used from a Barnstead NANOpure Diamond water instrument.

Note*: Care must be taken when handling KCN because it is a highly poisonous reagent and readily reacts with acids to generate the lethal HCN gas.*

Instrumental setup

A SpectraPOHORESIS 100 Modular Injector instrument from Thermo Separation Products was used for all analyses. A *ZETALIF* laser induced fluorescence detector from Picometrics was used with a MELES GRIOT 43 series ion laser power supply set to 488 nM wavelength. Fused silica capillaries were obtained from Polymicro Technologies Inc. Total length of capillary was 80 cm from inlet to outlet, with 50 cm effective length from inlet to detector. Buffers and electrophoretic voltage were varied depending on the experiment to be done and as defined in the specific runs.

Borate buffer (40 mM) was used as the running buffer for initial experiments and was adjusted to pH 10 using 0.1 M sodium hydroxide. In all CE-LIF experiments, electrophoretic potential difference/Voltage was set at a fixed value and therefore the

current could vary depending on the type or strength of buffer used. All samples were introduced into the capillary hydrodynamically by application of vacuum at the outlet of the capillary for a specified period of time. Running buffers were changed before every run. All samples were diluted using nanopure water after derivatization to a final concentration of 1 µM before analysis.

Sample derivatization, injection and analysis

Peptide samples were removed from the refrigerator and allowed 5 minutes to thaw. To 4 µL of peptide sample at a concentration of 1.25×10^{-4} M, 20 µL of 10 mM KCN dissolved in 10 mM borate buffer at pH 10 were added**.** 100 nanomoles of ATTO-TAG FQ™ were re-dissolved in 10 µL of methanol and vortexed to dissolve completely then pipetted into the sample micro-centrifuge tube which contained the mixture of peptide and KCN. This mixture was kept at room temperature for the next 60 minutes to effect derivatization. At the end of 60 minutes, the derivatized sample was diluted with nanopure water to stop the derivatization process and to lower the sample concentration to a predetermined value. The samples were then refrigerated at 4 °C awaiting analysis. Initial derivatization studies were done for a period of 90 minutes in order to determine an optimal derivatization time.

Samples were introduced into the capillary by hydrodynamic injection for periods 3 or 5 seconds depending on the experiment. Analysis was done at constant voltage with the anode set at the capillary inlet; current would therefore vary depending on the running buffer used. Initial analyses were done for 30 minutes to determine migration windows of

specific analytes. No migrating analytes were observed beyond 10 minutes and therefore typical analysis time was set at 15 minutes.

The amyloid beta peptides (40 and 42) were each analyzed separately to determine their migration times. Different buffer pH and strengths were analyzed in order to select an optimal buffer condition. Electrophoretic potential differences were also varied and the effect on retention time of the analytes noted in order to select an optimal electrophoretic potential difference. The electrophoresis buffer was then replaced with 10 nm bare (non- derivatized) gold nanoparticles suspended in buffer and the results recorded. Finally, analyses were done using 10 nm gold nanoparticles derivatized with an asymmetric disulfide.

Results and discussion

Results from capillary electrophoresis

In order to determine optimum derivatization time, amyloid beta peptides were derivatized by mixing 4 µL of peptide sample at a concentration of 1.25×10^{-4} M with 20 µL of 10 mM KCN dissolved in 10 mM borate buffer at pH 10 and 100 nM of ATTO-TAG FQ™ for 90 minutes then diluting the solution to a concentration of 1 µM with nanopure water. Samples were drawn from the derivatizing stock solution at 15 minute intervals for a total period of 90 minutes. Thus 6 samples in total were obtained and analyzed in order to determine an optimal time for derivatization. CE-LIF was used to measure the intensity of fluorescence in three replicates for each sample drawn. The derivatization time was plotted against average sample intensity.

Figure 14. Determination of optimal derivatization time for AB 40

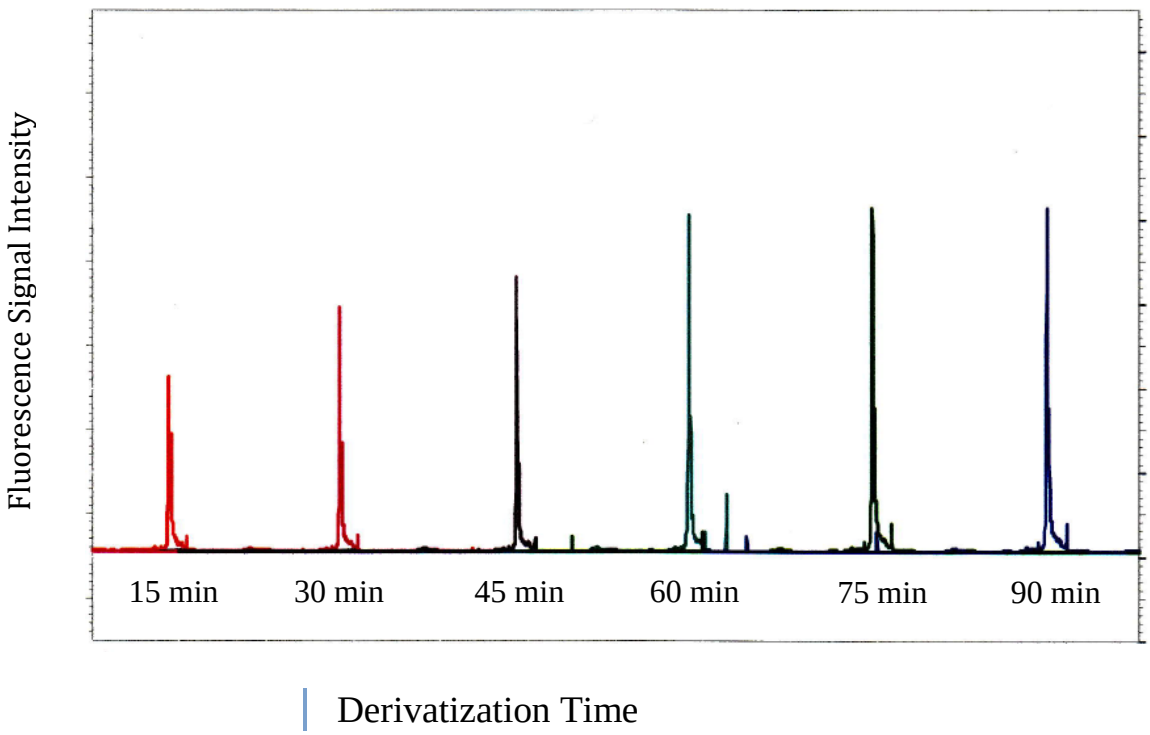

Shown in Figure 14 above are 6 chromatograms for Aβ 40 each being a representative of the replicates analysed after the specified duration of derivatization (15, 30, 45, 60. 75 and 90 minutes). The Y- axis shows the relative fluorescence intensity of the different samples. The electropherograms have been shifted on the X- axis for clarity.

Figure 15. Derivatization time of amyloid beta peptides against fluorescence intensity

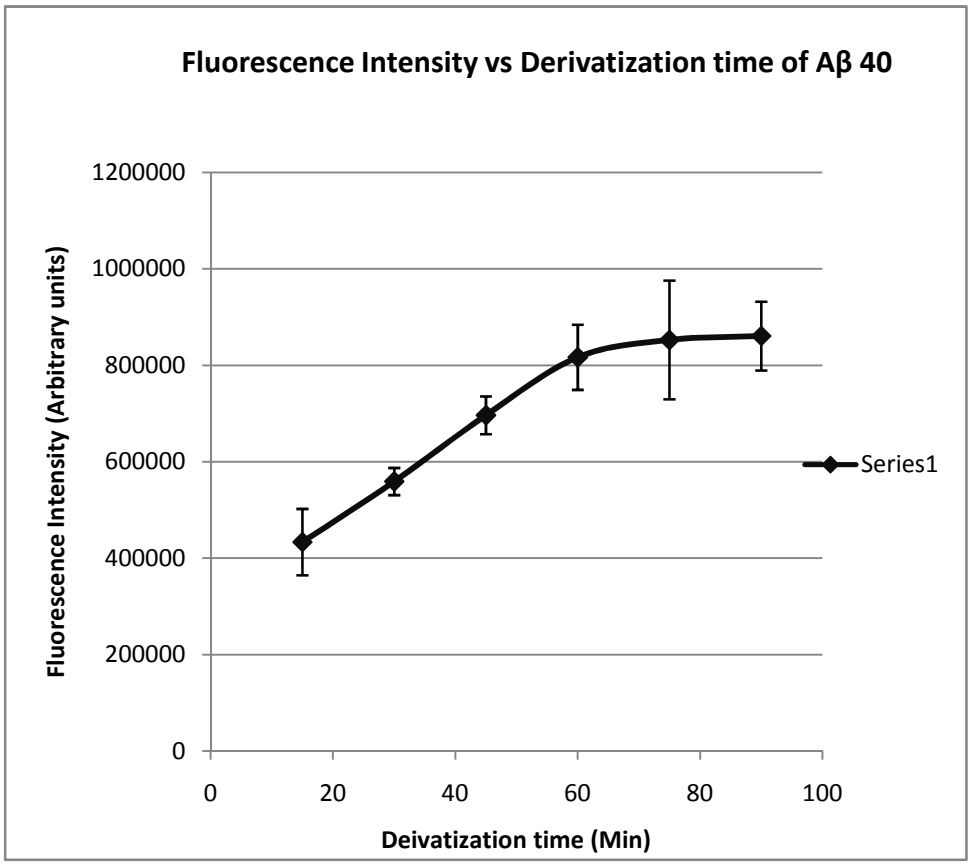

Figure 15 shows a plot of fluorescence intensity of the samples against the derivatization times. It was observed that the intensity of fluorescence increased steadily from the time of derivatization to about 60 minutes after which only minimal increments in fluorescence were observed. 60 minutes was therefore chosen as the optimal time for derivatization of the amyloid beta peptides.

Initial CE studies using borate buffer at different ionic strengths

Figure 16. Analysis of Aβ 42 (1 mM) performed in borate buffer (40 mM).

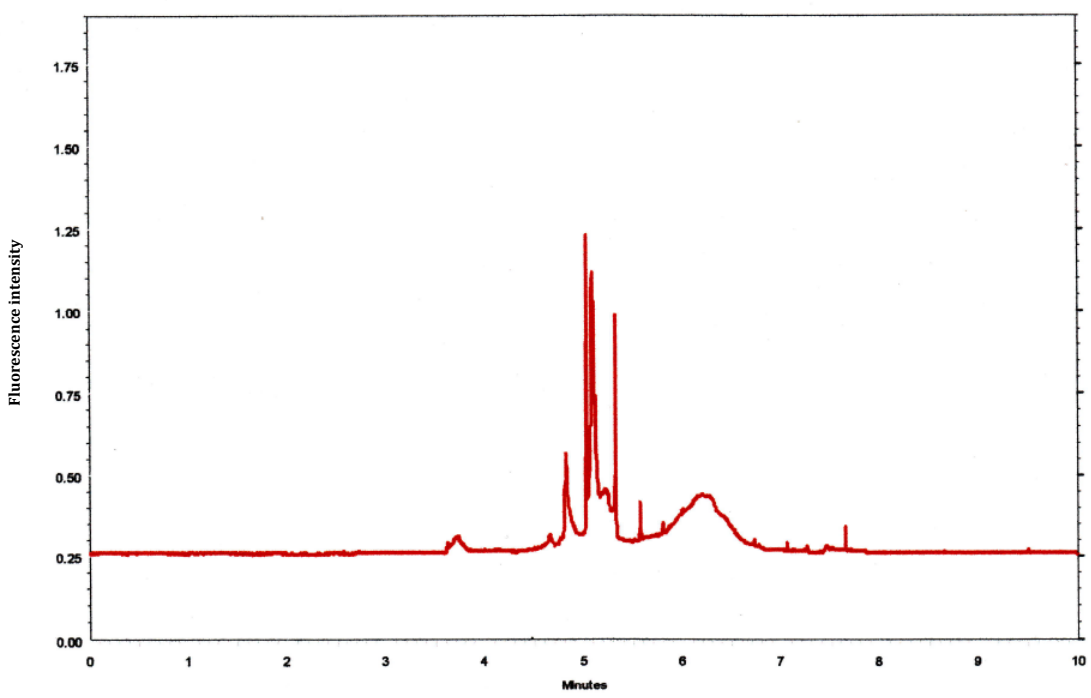

The voltage was set at 20 kV and a 5 second hydrodynamic injection. Numerous peaks were observed for the time between 4- 7 minutes, these peaks can be attributed to the aggregative behavior which is characteristic of amyloid beta peptides. It was also thought that the wide peak observed from 5-7 minutes could be suggestive of an overloaded column. Migration time of analytes is dependent on electrophoretic voltage

and buffer strength. The parameters above were therefore varied in order to obtain better electropherograms.

Calculation of injection volume

All hydrodynamic injections were done by application of 50 mbar (5.0103 kPa) suction pressure at the capillary outlet while dipping the inlet into a sample vial. The general equation for calculation of volume in vacuum injection is shown below.

$$V=\Delta P\pi d^4 t/128\eta L_t$$

Where V is injection volume, P is the pressure difference between the ends of the capillary, d is the inner diameter of the capillary, t is the injection time, η is the sample viscosity and L_t is the total length of the capillary. Assuming that the viscosity of the sample was 0.001 kg/ (m s) which is the viscosity of water, a 5 second injection in a capillary of total length of 80 cm at 50 mBar would be:-

$V=5000\ Pa \times 3.14\ (50 \times 10^{-6}\ m) \times 5\ s / 128 \times 0.001\ kg\ (m.s) \times 0.8 = 4.791 \times 10\text{-}^{12} m^3$

$= 4.79\ nL$

Because of the band broadening and peak tailing of the electropherogram in Figure 16 which are characteristics of an overloaded column, it was prudent to try smaller

injection volumes. All subsequent experiments were done using 3 second hydrodynamic injection unless noted otherwise. This corresponds to an injection volume of ~ 2.9 nL.

The electrophoretic voltage was increased to 25 kV and capillary length was maintained at 80 cm due to instrumentation setup. Effective length also remained at 50 cm to detector. The result is shown blow in Figure 17.

Figure 17. Analysis of Aβ 42 (1 mM) with 3 second hydrodynamic injection

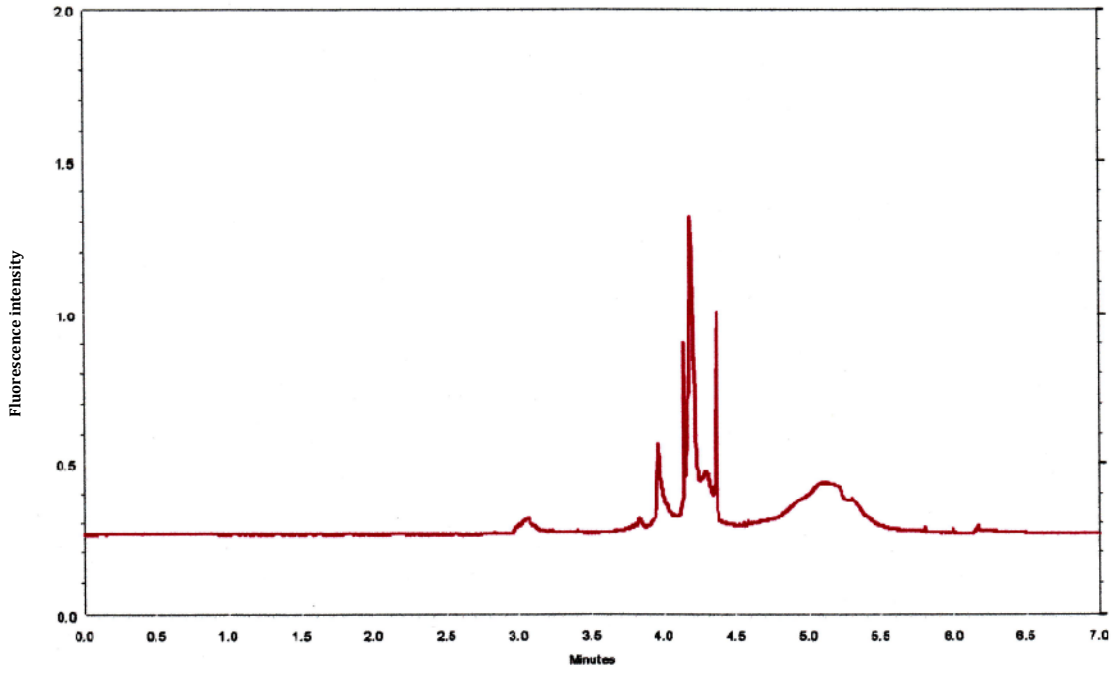

In the above electropherogram, the peak shapes of Aβ 42 with 3 second hydrodynamic injection and 25 kV electrophoretic voltage remained similar to the

previous trial with 5 second injection and 20 kV. The migration time however is shortened to 3-6 minutes due to the increment in electrophoretic voltage from 20 to 25 kV. The change in injection volume did not produce any significant change in the number of peaks observed.

Figure 18. Comparison of Aβ 42 analysis at different conditions

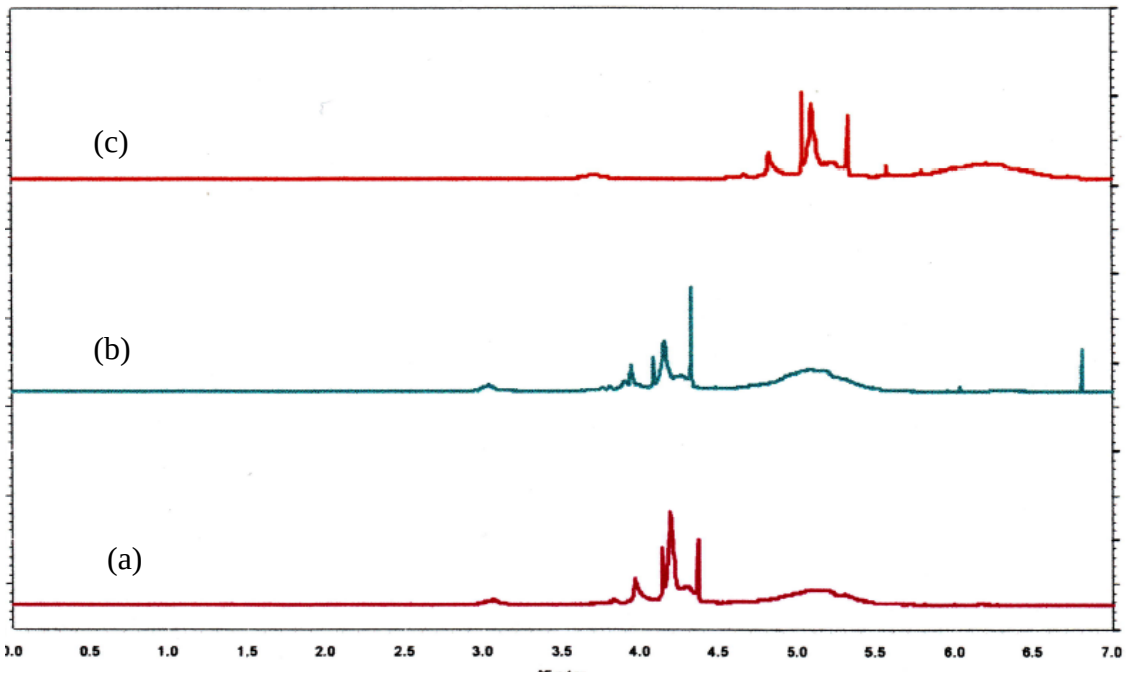

Figure 18 above shows the analysis of 1 mM Aβ 42 under three different conditions (a) 25 kV, 3 second injection (b) 25 kV, 5 second injection and (c) 20 kV with 5 second injection. The retention time decreases with increase in voltage but no remarkable change in peak shapes or peak numbers is evident.

Figure 19. Derivatized Aβ 40 performed in borate buffer (40 mM)

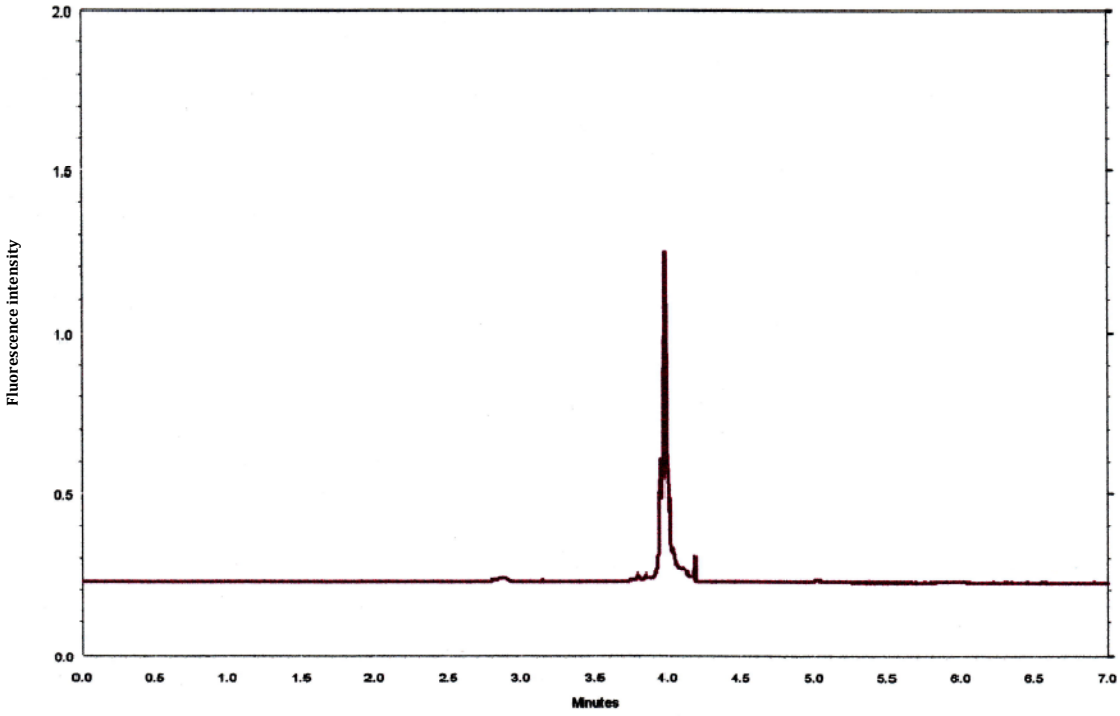

The voltage was set at 25 kV and a 5 second hydrodynamic injection was performed. The main peak for Aβ 40 appeared at 4.0 minutes with a smaller minor peak observed at around 4.2 minutes. As expected, the Aβ 40 peptides showed less aggregation compared to the Aβ 42 peptides which are more prone to the aggregation and is the main source of amyloid plagues in the brains of Alzheimer's disease patients. Nevertheless, the analyte peak is broad with an additional smaller peak that could have resulted from minor aggregation. Due to the large number of peaks observed for Aβ 42, a

separation of the two Alzheimer's disease peptides (Aβ 40 and Aβ 42) was not attempted using borate buffer since the analytes would be indistinguishable from the aggregates.

The band broadening and aggregation might have been enhanced by Joule heating due to the characteristic high conductivity currents of borate buffer. Joule heat is generated as a result of the flow of electric current through the electrophoresis buffer and is a major factor in the speed and resolution of separations.[42,43] It was therefore appropriate to explore the results obtained with other buffer solutions for comparison purposes. Zwitterionic buffers offer good conductivity at low currents and thereby contribute less to Joule heating. These buffers allow the use of higher voltages and thus can offer faster separations compared to other buffers. The effects on separation were monitored using *N*-cyclohexyl-3-aminopropanesulfonic acid (CAPS) which is a zwitterionic buffer. [44]

Figure 20. Analysis of Aβ 40 performed in CAPS buffer (40 mM)

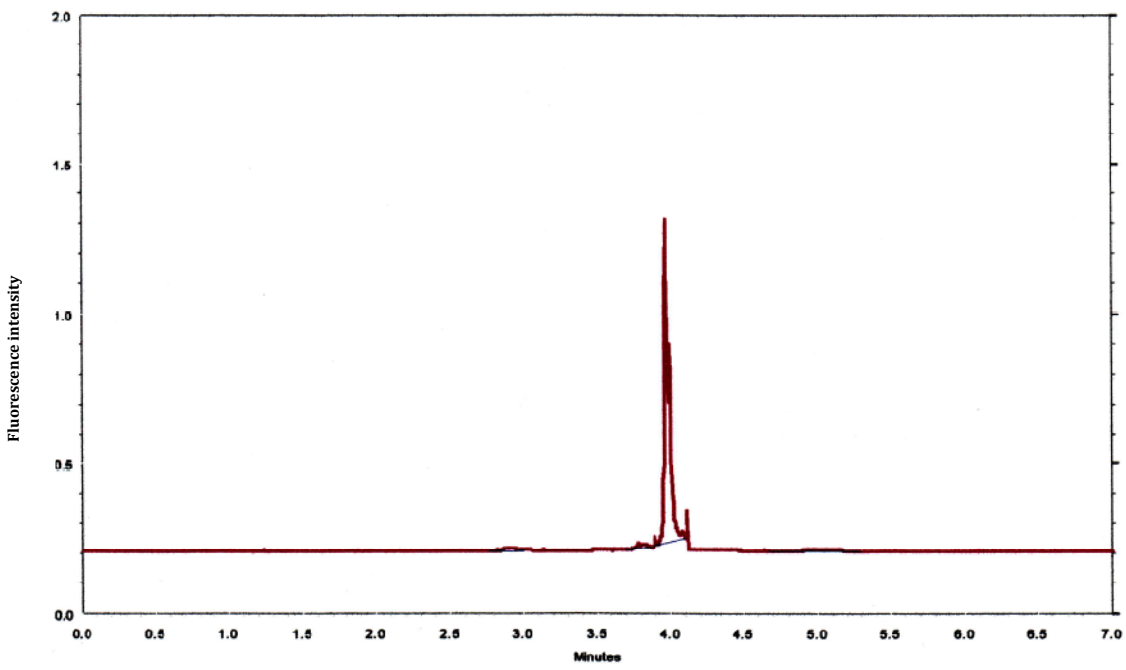

The above electropherogram of Aβ 40 in CAPS was obtained at a voltage of 25 kV and a 3 second hydrodynamic injection. This resulted in sharper and narrower peaks compared to the separation experiments using borate buffer. Some aggregation was evident but this was less than what had been previously observed when using borate as the running buffer.

Figure 21. Analysis of Aβ 42 performed in CAPS buffer (40 mM.

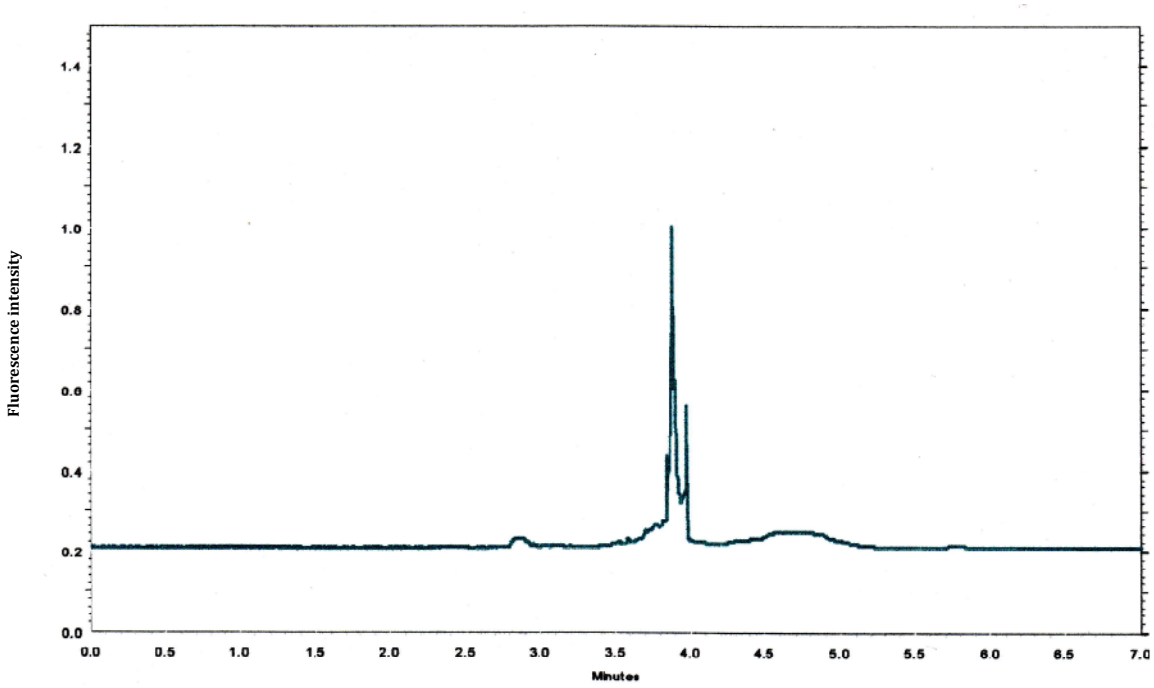

The electropherogram in Figure 21 was obtained at a voltage of 25 kV, 3 second hydrodynamic injection. In this figure, strong analyte fluorescence is observed around 3.9 minutes making up the main peak, a later smaller peak appearing at around 4 minutes is suggestive of aggregation of the analyte, the aggregation is however highly reduced compared to the studies done using borate as the running buffer.

Figure 22. Separate analyses of Aβ 40 and Aβ 42

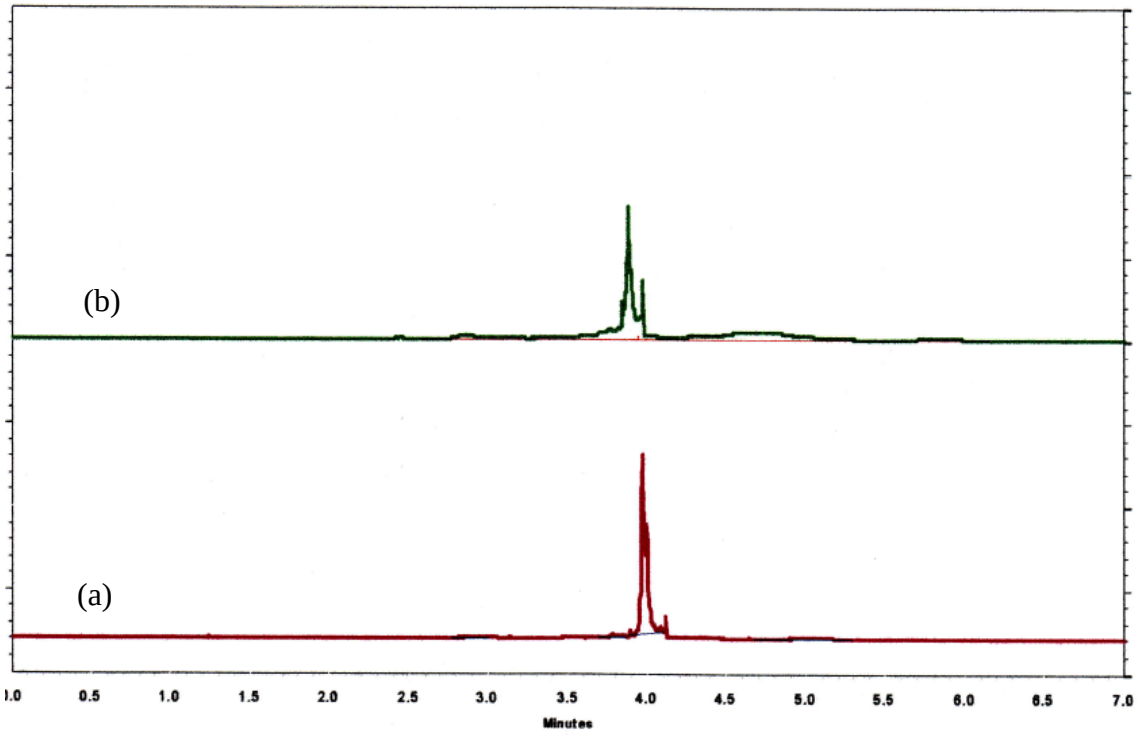

Electropherogram (a) represents an analysis of Aβ 40 using 40 mM CAPS buffer at 25 kV, 3 second hydrodynamic injection while (b) is Aβ 42 under the same conditions. It can be clearly seen that both peptides have very close migration times when subjected to similar electrophoretic conditions, a case that is explained by their close molecular weights and charge to size ratios.

The peptides were then derivatized separately as before then mixed together and diluted to a final concentration of 1 µM using nanopure water. The result of the separation is shown below in Figure 23.

Figure 23. Separation of amyloid beta peptides (Aβ 40 and Aβ 42)

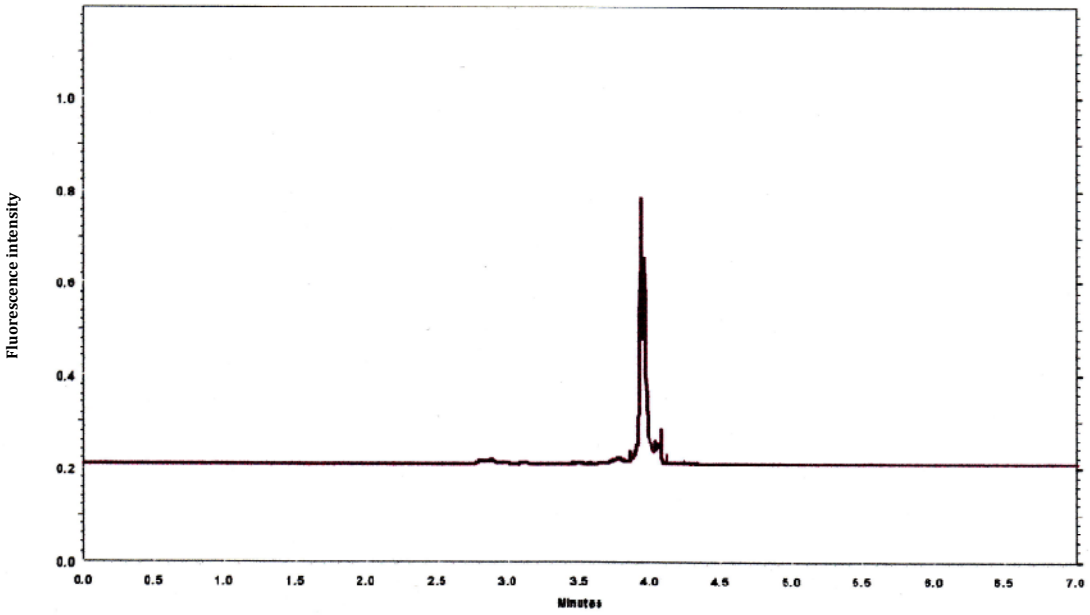

Figure 24. Expanded section of Figure 23

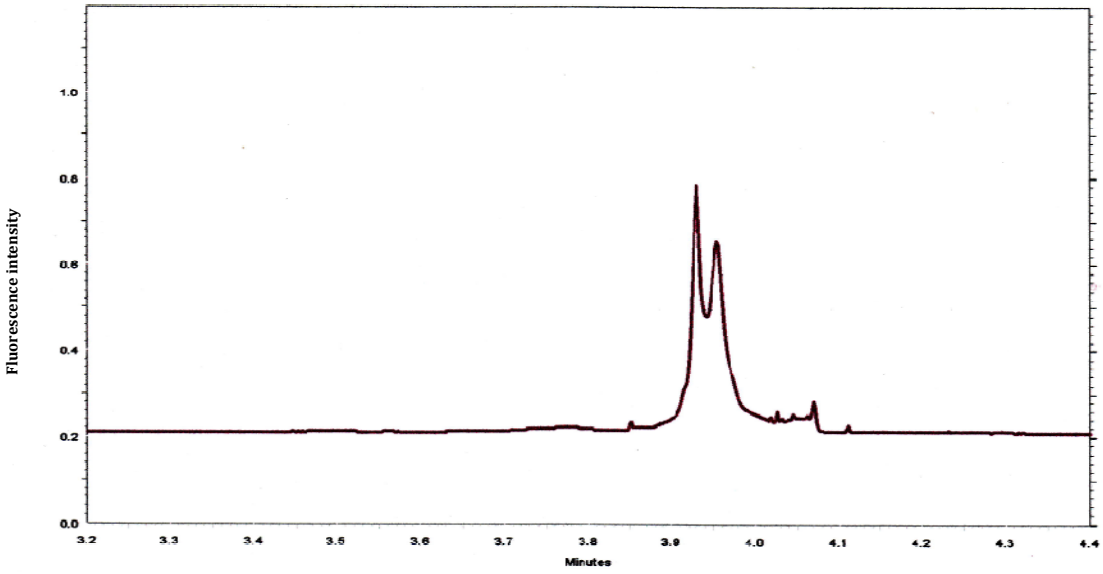

Some separation is evident as can be seen in the expanded section of Figure 24, however the separation has a poor resolution and the two analytes are indistinguishable.

Results using gold nanoparticles as a pseudo stationary phase

We further explored the separation of the two peptides in the presence of non derivatized gold nanoparticles. The gold nanoparticles were centrifuged and washed twice as explained under materials and methods. The nanoparticle pellet was then re-dissolved in 40 mM CAPS buffer which was used as a pseudo stationary phase in capillary electrophoresis experiments.

Figure 25 shows the separation of a mixture of Aβ 40 and Aβ 42 performed in 40 mM CAPS buffer at a voltage of 25 kV, 3 sec hydrodynamic injection in non-derivatized gold nanoparticles as a pseudo stationary phase.

Figure 25. Separation of Aβ 40 and Aβ 42 using bare gold nanoparticles

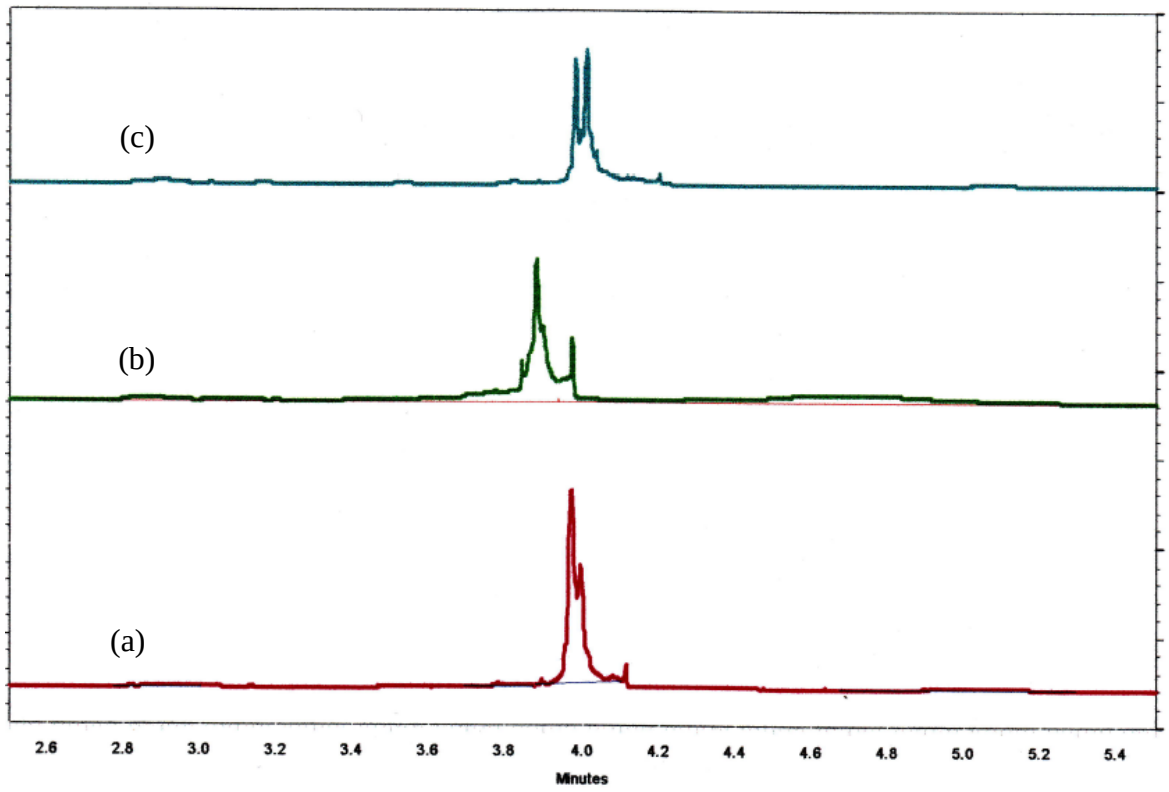

Figure 25 above shows separate analyses of (a) Aβ 40 (b) Aβ 42 and (c) a mixture of Aβ 40 and Aβ 42 all at a concentration of 1mM.

Figure 26. Expanded section of Figure 25

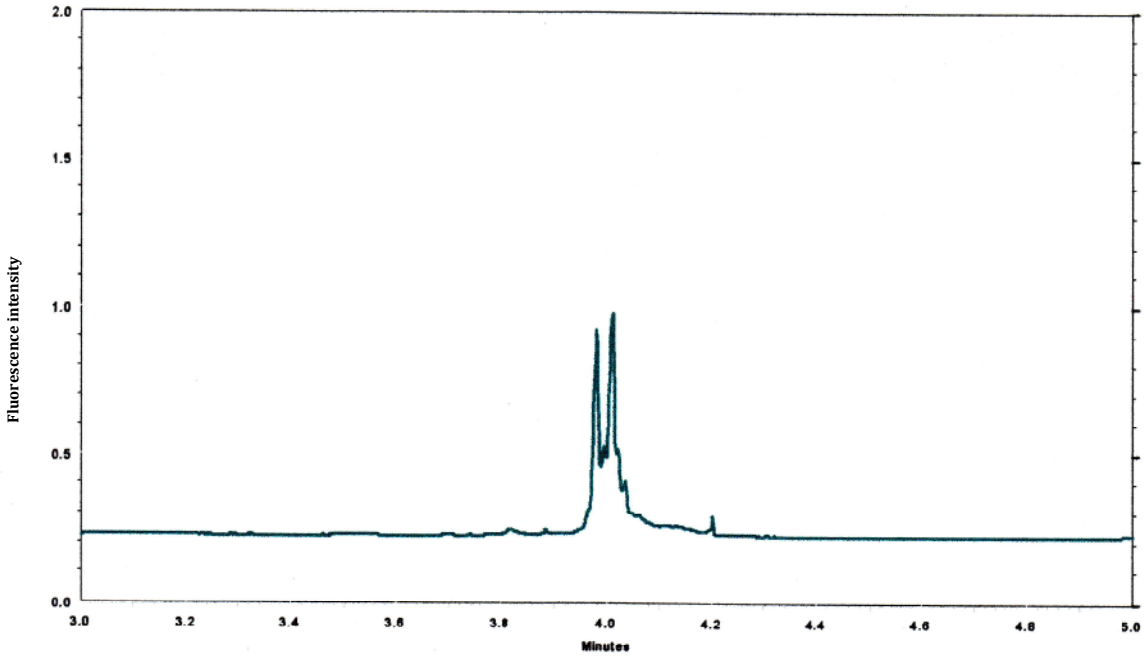

The inclusion of bare gold nanoparticles improved the resolution although differentiation and allocation of the peaks to their respective analyte could not be done without further information.

The next step was to perform the experiments in derivatized gold nanoparticles as the pseudo stationary phase. Separations were therefore done in fully derivatized 10 nm gold nanoparticles and the migration time of the two peptides determined. First the effect of injection time was revisited using Aβ 40. The result is shown in Figure 27.

Figure 27. Analysis of Aβ 40 at 5 and 3 second injection time

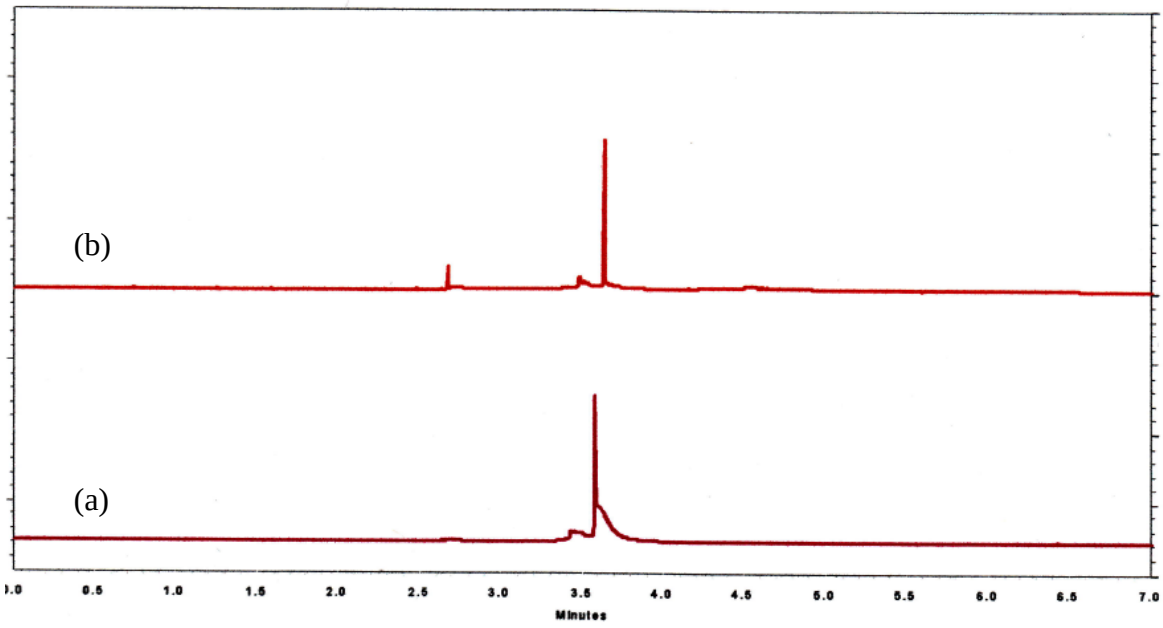

Figure 27 shows electropherograms of (a) Aβ 40 performed in 40 mM CAPS buffer at a voltage of 25 kV, 5 second hydrodynamic injection, and (b) Aβ 40 performed in 40 mM CAPS buffer at a voltage of 25 kV and at a reduced injection period of 3 seconds. Both analyses were performed in fully derivatized gold nanoparticles as a pseudo stationary phase in 40 mM CAPS buffer. As previously confirmed, analysis of Aβ 40 peptides with 5 second injections still showed peak tailing. It was therefore better to do the CE-LIF experiments with a 3 second injection time period. It was also noted that the peak shapes and migration time reproducibility was much better when experiments

were done with derivatized gold nanoparticles using CAPS buffer, compared to previous studies with borate, CAPS only or CAPS with bare gold nanopaticle analyses.

Both peptides were derivatized then mixed at equal proportions at the concentration of 1 µM for analysis. The migration times of the two peptides were then studied at 40 mM CAPS buffer, voltage of 25 kV, 3 seconds hydrodynamic injection in fully derivatized gold nanoparticles as a pseudo stationary phase and the results are shown in Figure 28.

Figure 28. Separate analysis of Aβ 40 and Aβ 42 in derivatized gold nanoparticles

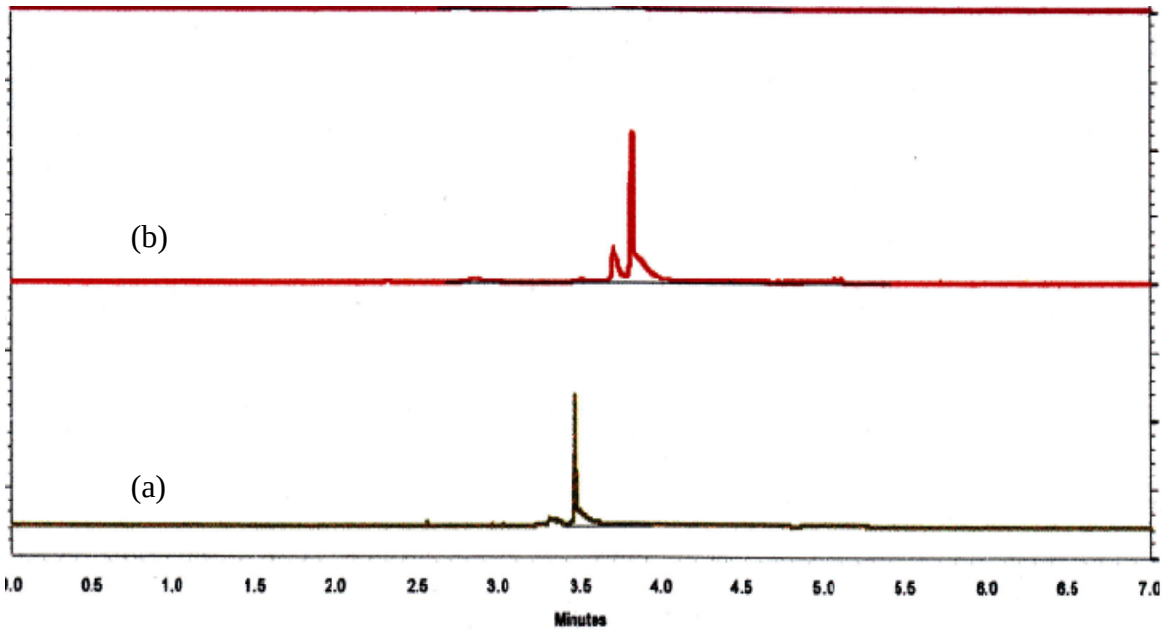

Figure 28 shows (a) electropherogram of Aβ 40 and (b) Aβ 42 in derivatzed gold nanoparticles. As can be seen in the Figure 28, Aβ 40 elutes at 3.5 minutes while Aβ 42 has a longer retention time under the same conditions and elutes at 4.0 minutes. This could be attributed to the difference in hydrophobicity and size of the two peptides. The difference between them is the two additional amino acids on Aβ 42 namely isoleucine and alanine that have hydrophobic side chains. These extra amino acids on Aβ 42 possibly increase the hydrophobic interactions of the peptide with the alkyl branches on the derivatized gold nanoparticles and thereby achieve a longer retention time.

Finally, having optimized the separations of each of the amyloid beta peptides, both peptides were mixed together after derivatization and diluted to a concentration of 1 µM. Analysis was performed with the electrophoretic conditions being 40 mM CAPS buffer pH 10, capillary length of 50 cm to detector, voltage of 25 kV, 3 sec hydrodynamic injection in fully derivatized gold nanoparticles as a pseudo stationary phase to give the results in Figure 29.

Figure 29. Analysis of a mixture of Aβ 40 and Aβ 42 in derivatized gold nanoparticles

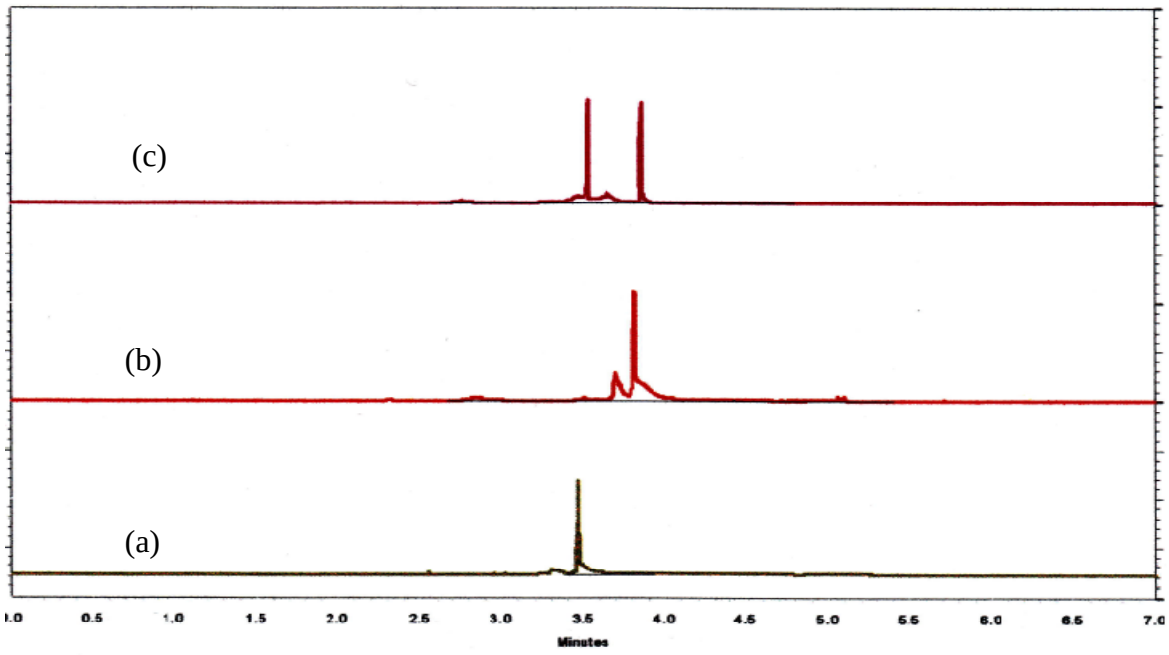

Figure 29 shows (a) analysis of Aβ 40, (b) Aβ 42 and (c) a mixture of Aβ 40 and Aβ 42. All analyses were done at a concentration of 1mM in 40 mM CAPS buffer with derivatized gold nanoparticles. A clear separation of both peptides is evident in (c) with Aβ 40 eluting first at 3.5 minutes, followed by Aβ 42 at 4.0 minutes, both peptides are well resolved.

Conclusion

Analysis of Aβ 42 in borate buffer with or without gold nanoparticles resulted in multiple peaks that could have been caused by aggregation of the analyte, leading to aggregates migrating at different times hence the multiple peaks. This was eliminated by changing the run buffer to CAPS; a zwitterionic buffer, which allows a good conductivity while reducing the effect of joule heating. The change in buffer also resulted in more reproducible peak shapes; however, peak tailing was evident. Tailing of the analyte peaks was eliminated by reduction of injection time from 5 seconds to 3 seconds.

Analysis of a mixture of Aβ 40 and Aβ 42 in CAPS both with and without gold nanoparticles resulted in poor resolution of the two amyloid beta peptides, however the resolution of both analytes was greatly increased when derivatized gold nanoparticles were used in the run buffer, suggesting that the derivatized gold nanoparticles interacted differently with each analyte to effect separation.

CHAPTER VI

CONCLUSION AND FUTURE WORK

Conclusion

It was successfully demonstrated in this work that by the use of derivatized gold nanoparticles, it is possible to exploit the difference in hydrophobicity of analytes to effect separation in capillary electrochromatography. The choice of ligands chemisorbed onto the gold nanoparticles is key to determining whether a separation would occur or not. A prior knowledge of the nature of the analytes involved would make the design of such specialized pseudo stationary phases easier and more relevant for specific applications.

Although CEC has to continuously compete with other separation technologies, it possesses several positive attributes including its small sample requirements, rapid and efficient separation among other advantages that if fully exploited can make it an extremely valuable technique.

Significance of the study

The use of biomarkers has become an accepted way for disease diagnosis, assessment of treatment efficacy and monitoring of disease progress. Clinicians can currently diagnose AD with 90% accuracy by using the knowledge of clinical and the

behavioral characteristics of the disease, however definitive diagnosis can only be done after an autopsy confirming tangles and senile plaques that are characteristic of AD.[6] Both Aβ 40 and Aβ 42 have been shown to be present in blood and cerebrospinal fluid of AD patients and can be used as reliable biomarkers of AD. Information obtained from assays of these amyloid peptides can be combined with cognitive assessments and neroimaging techniques to improve the diagnosis and monitoring of AD.

Future work

The mixed monolayer on gold nanoparticles studied in this work consisted of mercaptoundecanoic acid and dodecanethiol. These are however not the only compounds that can be used in the derivatization of gold nanoparticles. Other thiol terminated alkyl chains have also been successfully used in similar work.[35,36,37,41] It is interesting to further study the effect on separation of gold nanoparticles derivatized with other ligands. Different head groups other than carboxylic or methyl groups could also present interesting separation results.

Other than amyloid beta peptides, tau which is a microtubule associated protein involved in the assembly and stabilization of microtubules has been shown to be an Alzheimer's disease biomarker that can be used for diagnosis and tracking disease progression.[5] It would therefore be beneficial to study the separation of both the amyloid beta peptides and the tau proteins to better understand the relationship between the different biomarkers.

Quantitation work of the biomarkers in artificial cerebrospinal fluid can give an insight into the complexity of the separation and provide useful information on sample clean up procedures that may be required before sample analysis. Such work would optimize separation conditions for analysis of patient samples.

Ultimately the goal is to develop a capillary electrochromatography technique that can be used for the clinical analysis of samples from patients suffering from Alzheimer's disease and be able to accurately diagnose the disease based on the information obtained from the concentration of the different biomarkers in the shortest time possible and at a cost effective way.

REFERENCES

1. Aluise, C. D.; Sowell, R. A.; Butterfield, D. A. Peptides and proteins in plasma and cerebrospinal fluid as biomarkers for the prediction, diagnosis, and monitoring of therapeutic efficacy of Alzheimer's disease, *Biochimic. et Biophys. Acta.* **2008**, 1782, 549–558.
2. Alzheimer's Association. Alzheimer's disease facts and figures 2007, *Alzheimer's Association*. **2007**.
3. Brookmeyer, R.; Johnson, E.; Ziegler-Graham, K.; Arrighi, H. M. Forecasting the global burden of Alzheimer's disease, *Alzheimer's and Dementia*. **2007**, 3,186-191.
4. Marum, R. J. Current and future therapy in Alzheimer's disease. *Fund. & Clin. Pharmacol.* **2008**, 22, 265–274.
5. U.S. Department of Health and Human Services, AD research advances: Many paths to the goal, **2005-2006** progress report on Alzheimer's disease.
6. Kabanov, A.V.; Gendelman, H.E. Nanomedicine in the diagnosis and therapy of neurodegenerative disorders, *Prog. Polym. Sci*. **2007**, 32, 1054–1082.
7. Wang, D. S.; Dickson, D. W.; Malter, J. β-amyloid degradation and Alzheimer's disease. *J. of Biomed. and Biotechn.* **2006**, 1-12.

8. Rauk, A. Why is the amyloid beta peptide of Alzheimer's disease neurotoxic? *The Royal Soc. of Chem. - Dalton Trans.* **2008**, 1273–1282.
9. Oe, T.; Ackermann, B. L.; Inoue, K.; Berna, M. J.; Garner, C. O.; Gelfanova, V.; Dean, R. A.; Siemers, E. R.; Holtzman, D. M.; Farlow, M. R.; Blair, I. A. Quantitative analysis of amyloid β peptides in cerebrospinal fluid of Alzheimer's disease patients by immunoaffinity purification and stable isotope dilution liquid chromatography/negative electrospray ionization tandem mass spectrometry, *Rapid Commun. Mass Spectrom*. **2006**, 20, 3723–3735.
10. Wiltfang, J.; Esselmann, H.; Bibl, M. *et al.* Amyloid β peptide ratio 42/40 but not Aβ42 correlates with phospho-Tau in patients with low- and high- CSF Aβ40 load. *J. of Neurochem.* **2007**, 101, 1053–1059.
11. Oijen, M.; Hofman, A.; Soares, H. D.; Koudstaal, P. J.; Breteler, M. M. Plasma Aβ1–40 and Aβ1–42 and the risk of dementia: a prospective case-cohort study *Lancet Neurol.* **2006**; 5: 655-660.
12. Spillantini, M. G.; Goedert, M. Tau protein pathology in neurodegenerative Diseases, *Trends Neurosci*. **1998**, 21, 428-433.
13. Hampel, H.; Goernitz, A.; Buerger, K. Advances in the development of biomarkers for Alzheimer's disease: from CSF total tau and Aβ1–42 proteins to phosphorylated tau protein, *Brain Res. Bull.* **2003**, 61, 243-253.
14. Sunderland, T.; Mirza, N.; Putnam, K. T; Linker, G.; Bhupali, B.; Durham, R.; Soares, H.; Kimmel, L.; Friedman, D.; Bergeson, J.; Csako, G.; Levy, J. A.; Bartko, J. J.; Cohen, R. M. Cerebrospinal Fluid β-Amyloid1-42 and Tau in

Control Subjects at Risk for Alzheimer's Disease: The Effect of APOE ε4 Allele. *Biol Psychiatry*. **2004**, 56, 670-676.

15. Varesio, E.; Rudaz, S.; Krause, K.; Veutheya, J. Nanoscale liquid chromatography and capillary electrophoresis coupled to electrospray mass spectrometry for the detection of amyloid-β peptide related to Alzheimer's disease. *J. of Chromatogr*. **2002**, 135–142.
16. Clarkea, N. J.; Tomlinsona, A. J.; Ohyagib, Y.; Younkinc, S.; Naylord, S. Detection and quantitation of cellularly derived amyloid β peptides by immunoprecipitation-HPLC-MS. *FEBS Letters*. **1998**, 430, 419-423.
17. Kato, M.; Kinoshita, H.; Enokita, M.; Hori, Y.; Hashimoto, T.; Iwatsubo, T.; Toyo'oka, T. Analytical Method for β-Amyloid Fibrils Using CE-Laser Induced Fluorescence and Its Application to Screening for Inhibitors of β-Amyloid Protein Aggregation. *Anal. Chem*. **2007**, 79, 4887-4891.
18. Nilsson, C.; Birnbaum, S.; Nilsson, S. Use of nanoparticles in capillary and microchip electrochromatography. *J. of Chromatogr. A*, **2007**, 1168, 212–224.
19. Liu, F.; Hsu, Y.; Wu, C. Open tubular capillary electrochromatography using capillaries coated with films of alkanethiol-self-assembled gold nanoparticle layers. *J. of Chromatogr. A*, **2005**, 1083, 205–214.
20. Jac, P.; Polasek, M.; Pospisilova, M. Recent trends in the determination of polyphenols by electromigration methods. *J. of Pharm. and Biomed. Anal*. **2006**, 40, 805–814.

21. Gottlicher, B.; Bachmann, K. Application of particles as pseudo-stationary phases in electrokinetic Chromatography. *J. of Chromatogr. A*, **1997**, 780, 63-73.

22. Terabe, S.; Otsuka, K.; Ichikawa, K.; Tsuchiya, A.; Ando, T. Electrokinetic Separations with Micellar Solutions and Open-Tubular Capillaries. *Anal. Chem.* **1984**, 56, 113-116.

23. Neiman, B.; Grushka, E.; Lev, O. Use of Gold Nanoparticles To Enhance Capillary Electrophoresis. *Anal. Chem.* **2001**, 73, 5220-5227.

24. Guihen, E.; Glennon, J. D. Nanoparticles in Separation Science: Recent Developments. *Anal. Lett.* **2003**, 36, 3309-3336.

25. Pumera, M.; Wang, J.; Grushka, E.; Polsky, R. Gold Nanoparticle-Enhanced Microchip Capillary Electrophoresis, *Anal. Chem.* **2001**, 73, 5625-5628.

26. Yu, C.; Su, C.; Tseng, W. Separation of Acidic and Basic Proteins by Nanoparticle-Filled Capillary Electrophoresis. *Anal. Chem.* **2006**, 78, 8004-8010.

27. Yang, L.; Guihen, E.; Glennon, J. D. Alkylthiol nanoparticles in sol-gel open tubular capillary electrochrmatography. *J. Sep. Sci.* **2005**, 28, 757–766.

28. Shon, Y.; Mazzitelli, C.; Murray, R. W. Asymmetrical Disulfides and Thiol Mixtures Produce Different Mixed Monolayer-Protected Gold Clusters. *Langmuir*, **2001**, 17, 7735-7741.

29. O'Mahony, T.; Owens, V. P.; Murrihy, J. P; Guihen, E.; Holmes, J. D.; Glennon, J. D. Alkylthiol gold nanoparticles in open-tubular capillary Electrochromatography. *J. of Chromatogr. A.* **2003**, 1004, 181–193.

30. Biebuyck, H .A; Whitesides, G. M. Interchange between Monolayers on Gold Formed from Unsymmetrical Disulfides and Solutions of Thiols: Evidence for Sulfur-Sulfur Bond Cleavage by Gold Metal. *Langmuir,* **1993**, 9, 1766-1770.
31. Clarke, N, J; Crow, F, W; Younkin, S; Naylor, N. Analysis of *in Vivo*-Derived Amyloid-β Polypeptides by On-Line Two-Dimensional Chromatography-Mass Spectrometry. *Anal. Biochem.* **2001**, 298, 32–39.
32. Craig, D. B; Polakowski, R. M; Arriaga, E; Wong, J. C; Ahmadzadeh, H; Stathakis, C; Dovichi, N. J; Sodium dodecyl sulfate-capillary electrophoresis of proteins in a sieving matrix utilizing two-spectral channel laser-induced fluorescence detection. *Electrophoresis*, **1998**, 19, 2175-2178.
33. Dawson, G. B.; Matyska, M. T.; Pesek, J. J.; Seipert, R. R. Electro-chromatographic studies of etched capillaries modified with a cyano pentoxy biphenyl liquid crystal *J. of Chromatogr. A.* **2004**, 1047, 299–303.
34. Zhang, Z.; Yan, B.; Liao, Y.; Liu, H. Nanoparticle: is it promising in capillary electrophoresis? *Anal. Bioanal. Chem.* **2008**, 391, 925–927.
35. Bain, C. D.; Troughton, E. B.; Tao, Y. T.; Evall, J.; Whitesides, G. M.; Nuzzo, R. G. Formation of monolayer films by the spontaneous assembly of organic thiols from solution onto gold. *J. Am. Chem. Soc.* **1989**, 111, 321-335.
36. Lin S, Y.; Tsai, Y.; Chen, C.; Lin, C.; Chen, C. Two-step derivatization of neutral and positively charged thiols onto citrate-stabilized Au nanoparticles. *J. Phys. Chem. B.* **2004**, 108, 2134-2139.

37. Mayya, K, S; Schoeler , B.; Caruso, F. Preparation and Organization of Nanoscale Polyelectrolyte-Coated Gold Nanoparticles, *Adv. Funct. Mater*. **2003**, 13, 183-188.

38. Cha, S.; Kim, K.; Kim, J.; Lee, W.; Lee, J. Thermal Behavior of Gold (I) − Thiolate Complexes and Their Transformation into Gold Nanoparticles under Heat Treatment Process. *J. Phys. Chem. C.* **2008**, 112, 13862–13868.

39. Kawasaki, M.; Sato, T.; Tanaka, T.; Yamada, R.; Wano, H.; Uosaki, K. Effect of Temperature on Structure of the Self-Assembled Monolayer of Decanethiol on Au (111) Surface, *Langmuir*, **2000**, 16, 5523-5525.

40. Kawasaki, M.; Sato, T.; Tanaka, T.; Takao, K. Effects of concentration and temperature on the formation process of decanethiol self-assembled monolayer on Au (111) followed by electrochemical reductive desorption. *Langmuir*, **2000**, 16, 1719–1728.

41. Love, J, C.; Estroff, L, A.; Kriebel, J, K.; Nuzzo, R, G; Whitesides, G, M. Self-Assembled Monolayers of Thiolates on Metals as a Form of Nanotechnology, *Chem. Rev*. **2005**, 105, 1103-1169.

42. Heiger D.; N. High Performance Capillary Electrophoresis: An Introduction, France: Hewlett Packard Company, **1992**, 30.

43. Xuan, X.; Li, D. Joule heating effects on peak broadening in capillary zone electrophoresis. *J. Micromech. Microeng.* **2004**, 14, 1171–1180.

44. Haddad, P. R.; Evenhuis, C, J. Joule heating effects and the experimental determination of temperature during CE. *Electrophoresis*, **2009**, 30, 897–909.

45. McLaren, D, G.; Chen, D, D. A quantitative study of continuous flow counterbalanced capillary electrophoresis for sample purification. *Electrophoresis*, **2003**, 24, 2887–2895

46. Kambhampati, D.K.; Knoll, W. Surface-plasmon optical techniques, *Curr. Opin. Colloid* & *Inteface Sci.* **1999**, 4, 273-280.

47. Li, X.; Jiang, L.; Zhan, Q.; Qian, J.; He, S. Localized surface plasmon resonance (LSPR) of polyelectrolyte-functionalized gold-nanoparticles for bio-sensing. *Colloids and Surfaces A: Physicochem. Eng. Aspects*. **2009**, 332 ,172–179.

48. Jin, Y. *et al.* Gold nanoparticles prepared by sonochemical method in thiol-functionalized ionic liquid. *Colloids and Surfaces A: Physicochem. Eng. Aspects*. **2007**, 302, 366–370.

49. Dovichi, N, J. *et al.* Reaction of fluorogenic reagents with proteins I. Mass spectrometric characterization of the reaction with 3-(2-furoyl)quinoline-2-carboxaldehyde, Chromeo P465, and Chromeo P503. *J. of Chromatogr. A.* **2008**, 1194, 243–248

50. Dumke, J. C; Nussbaum, M. A. Adaptation of a Commercial Capillary Electrophoresis Instrument for Chemiluminescence Detection. *Anal.Chem.* **2007**, 79, 1262-1265.

51. Oilman, S. D; Ewing, A. O. Analysis of Single Cells by Capillary Electrophoresis with On-Column Derivatization and Laser-induced Fluorescence Detection. *Anal. Chem.* **1995**, 67, 58-64.